ABSTRACT

REMOVAL OF GASOLINE-BASED HYDROCARBONS BY VAPOR PERMEATION MEMBRANES

by
Shivashanker Bagavandoss

Removal and recovery of evaporated lighter gasoline fractions can be effectively implemented by selectively permeating the hydrocarbons (HCs) and other volatile organic compounds (VOCs) from the vented air streams through nonporous hydrophobic polymeric membranes subjected to vacuum on the permeate side and then condensing these organics from the permeate. Such a vapor permeation process employing spiral-wound membranes has already been commercialized for VOCs. In this study, attention has been focused on removal of hydrocarbons from nitrogen flowing through the bore of microporous hydrophobic hollow fibers with a specially engineered nonporous silicone coating on the outside surface with a view to reducing the HC concentration in treated gas stream from 17% to the lowest desirable level. Membrane modules containing such hollow fibers possess 7-10 times more surface area per unit volume, have higher selectivities to hydrocarbons and lowered air flux due to the flow configuration, pore condensation and the membrane type. Studies with an inert liquid immobilized in the substrate pores of the membranes (ILM) have shown very high selectivities compared to the composite membrane. A mathematical model has been developed to explain the permeation-separation behavior of the hydrocarbons and the VOCs as well. A novel aspect of the model is the effort made to illustrate and explain the difference between the two modes of introduction of the feed viz. shell-side and tube-side.

REMOVAL OF GASOLINE-BASED HYDROCARBONS
BY VAPOR PERMEATION MEMBRANES

by
Shivashanker Bagavandoss

A Thesis
Submitted to the Faculty of
New Jersey Institute of Technology
in Partial Fulfillment of the Requirements for the Degree of
Masters of Science in Chemical Engineering

Department of Chemical Engineering,
Chemistry and Environmental Science

October 1996

APPROVAL PAGE

REMOVAL OF GASOLINE-BASED HYDROCARBONS
BY VAPOR PERMEATION MEMBRANES

Shivashanker Bagavandoss

Dr. Kamalesh K. Sirkar, Thesis Advisor   Date
Professor of Chemical Engineering
New Jersey Institute of Technology

Dr. Angelo S. Perna, Committee Member   Date
Professor of Chemical Engineering
New Jersey Institute of Technology

Dr. Robert G. Luo, Committee Member   Date
Assistant Professor of Chemical Engineering
New Jersey Institute of Technology

BIOGRAPHICAL SKETCH

Name: Shivashanker Bagavandoss

Degree: Master of Science

Date: October 1996

Date of birth:

Place of birth:

Undergraduate and Graduate Education:

- Masters of Science in Chemical Engineering,
  New Jersey Institute of Technology, Newark, NJ, 1996

- Bachelor of Science in Chemical Engineering,
  Birla Institute of Technology and Science, Pilani, India, 1994

Major: Chemical Engineering

ACKNOWLEDGEMENT

TABLE OF CONTENTS

TABLE OF CONTENTS
(Continued)

LIST OF TABLES

LIST OF FIGURES

LIST OF FIGURES
(Continued)

CHAPTER 1

INTRODUCTION

1.1 Treatment of Organic Compounds

Separation processes play a crucial role in the chemical process industries. They serve a range of purposes like removal of contaminants from raw materials, purification of products and elimination of pollutants from liquid and gas streams. These processes are extremely essential from an economic perspective. A number of separation processes like distillation, extraction, adsorption and a variety of membrane separation processes have been in use in industries (Humphrey et al., 1995). Contaminants usually treated by these processes are either pollutants or organic solvents which have significant commercial value. Many industrial processes use organic solvents as carrier or dissolving agents. During such operations, volatile organic compounds (VOCs) escape into the atmosphere through exhaust air streams. Until 1970, these streams were routinely discharged to the atmosphere since regulations for pollutant emission were essentially non-existent. Intensive studies have proved that these compounds and other hydrocarbons have a hazardous effect on human life. Hydrocarbons, in particular, have been found to cause cancer and in the presence of nitrogen oxides and sunlight, react to form a photochemical smog which is a potential threat to the environment. Stringent regulations in the present decade, mainly, the Clean Air Act Amendments of 1990 (CAAA), have forced industries to focus their attention on pollution prevention and control of emissions. A study by the U.S. Environmental Protection Agency (EPA) shows that approximately 2 million tons

of organic solvents are emitted from coating facilities every year (Deng et al., 1995). Thousands of currently regulated and unregulated sources will have to seek more efficient control strategies to reduce emissions and comply with better air quality standards. Also, it is economically desirable to recover and reuse these solvents. Hydrocarbons lost through petroleum vapor emissions are of particular importance to this thesis.

A number of physical and chemical processes can be used to separate or destroy these volatile organics/ hydrocarbons. Commonly used techniques are incineration, condensation, liquid absorption or activated-carbon adsorption.

Incineration is not considered very economical due to the dilute concentration of organics in the air and due to the formation of chlorinated compounds like dioxins. Organics in these petroleum vapor emissions can also be recovered by condensing the whole air stream at atmospheric pressure using suitable refrigerants, but the energy and capital costs are very high. Problems associated with absorption are high costs for large or small flow rates, bulkiness of equipment and flooding. For adsorption, a large amount of activated carbon would be required for high concentrations. Presence of water vapor, ketones, aldehydes and ethers render the process less efficient besides operational problems like contamination of carbon bed and equipment corrosion. This situation is deemed ideal for membrane separation processes.

The potential for removing hydrocarbons from air by membrane separation processes is being explored increasingly. These processes are simple and reliable. For a greater degree of separation, the membrane, which is the major component in the membrane-based separation system, should have high permeability for the vapor component, high selectivity between gas/vapor components and high chemical, thermal

and mechanical stability. The basic advantages membrane technology has over conventional processes are the modular nature of membrane devices, high surface area per unit volume of the modules and no need for a second phase. Although separation of gas mixtures has been under investigation for a long time (Sengupta and Sirkar, 1986), efforts to separate hydrocarbons and VOCs from air/N_2 using polymeric membranes began recently.

A number of transport mechanisms can be used to separate vapors from air. The transport-cum-separation mechanisms are identified as follows (Sengupta and Sirkar, 1986):

1. Poiseuille flow

2. Knudsen flow

3. Surface diffusion

4. Pore condensation

5. Pore blockage

6. Permeation (solution-diffusion).

Membranes employing the first five transport mechanisms can be either porous or microporous depending on the pore size in the membrane matrix, gas pressure and temperature. Membranes with permeation as the separation mechanism are nonporous. This study is focused on vapor separation process based on the mechanism of vapor permeation in a composite membrane. Vapor permeation through nonporous membranes is studied on the basis of the solution-diffusion model. The mechanism depends on the nature of the membrane i.e. whether it is glassy (solid-like), rubbery (liquid-like) or gel (semi-solid/ semi-liquid). Glassy polymers facilitate the removal of small molecules of

gases like H_2 and He through the small openings between rigid polymer backbones rather than gaseous species with large diameters like organic solvents. Therefore rubbery polymeric membranes (instead of glassy) are normally used for VOC permeation-based separation.

1.2 Polymer Membranes

The permeation of a gas/vapor through a dense rubbery polymeric membrane depends on the diffusion coefficient and the solubility coefficient of the gas/vapor in the polymer. Generally, the diffusion coefficient of a molecule decreases with increasing molecular size, but the solubility coefficient increases with increasing molecular size and with increasing condensibility of the gas/vapor molecules. Ease of molecular transport is determined more by the solubility coefficient than by the diffusion coefficient. The high solubility of organic vapors in rubbery polymers is the reason for their high permeability.

Experiments conducted by Baker et al. (1987) for the separation of nitrogen and organic vapors using various polymer membranes established that permeabilities of VOCs (toluene, acetone etc.) increase with increasing vapor pressure in the gas phase. Among these membranes, silicone rubber showed the highest selectivity for toluene/N_2 and acetone/N_2. Strathmann et al. (1986) developed composite membranes using poly(dimethylsiloxane) as the selective barrier both in the form of hollow fibers and flat sheets to study the permeation/separation behaviour of VOCs.

Kimmerle et al. (1988) carried out similar investigations using polysulfone hollow fibers with poly(dimethylsiloxane) laminated to the inner surface. Wijmans and Helm (1989) used MTR (Membrane Technology & Research, Menlo Park, CA) membranes

assembled in spiral-wound units for separation of organic vapors from N_2.

Although silicone (poly(dimethylsiloxane)) membranes exhibit high permeabilities for various VOCs and have been used in a number of studies, yet the overall membrane configurations and modules explained above are not very efficient. For example, the porous substrate used by Kimmerle et al. (1988) had a low porosity; this resulted in a very low value of permeability coefficient and a high value of effective membrane thickness. These quantities adversely affect the VOC flux through the membrane, all other conditions remaining constant. MTR-based membranes are flat and have to be supported. They are packed into a module using the spiral wound configuration (Baker et al., 1987; Wijmans and Helm, 1989). The membrane surface packing density (area per unit volume) of the spiral-wound membrane module is much lower than that possible in a hollow fiber module resulting in lower separation processing capacity per unit volume.

Cha (1994) used ultrathin silicone membranes bonded to microporous polypropylene substrate by plasma polymerization. Hollow fiber module configuration was used to achieve permeation/separation of methanol and toluene from a N_2-VOC mixture. The study demonstrated that this configuration is highly efficient. A mathematical model was formulated to describe the experimental separation behavior, but limited attempts were made to simulate the model due to the absence of a relation between the permeance of the VOC and its concentration and due to the need for more experimental data points to check the validity of the model. Malik (1995) had carried out some experiments to determine the variation of permeance with VOC concentration for toluene and methanol and the separation behavior of other VOCs (viz. methylene chloride, acetone, hexane etc.). Subtle modifications of the pre-designed permeation

experiment, like separation of VOCs at feed pressures higher than atmospheric and introduction of feed from the shell side (with tube side under vacuum) instead of the more efficient tube side feed mode, were also studied very briefly.

Emissions from gasoline storage tanks are of particular interest in this study. A large amount of the lighter fractions of petroleum products is emitted as vapors from ocean tankers and storage tanks during storage, transfer and loading of petroleum products. These emissions are both, a health hazard and an economic loss. Gasoline and other light hydrocarbon emissions are also of importance. Recovery of evaporated gasoline has been under serious investigation for the past few years. Comprehensive analysis of a typical sample of emission from these tanks and other sources has established the primary components to be C_4-C_6 alkanes, present at the level of 17-24% (Ohlrogge et al., 1990). Hence, attention has been focused on the removal of these three hydrocarbons (butane, pentane and hexane) only.

In this investigation, efforts have been made to study the permeation behaviour of three hydrocarbons; butane, pentane and hexane. These are the primary components of vapor emissions for gasoline. Recovering them would be highly useful. Attempts to study permeation in an immobilized membrane are a unique part of this study. A mathematical model to demonstrate the difference between shell-side and tube-side feed, if any, has also been developed.

In this study, a gas mixture containing ~ 12% Butane, ~ 4% Pentane, ~ 1% Hexane and ~ 83% Nitrogen was chosen as the feed. The choice of this composition is based on the analysis of a typical sample of off-gas from gasoline storage tanks (Ohlrogge et al., 1990), which revealed the presence of C_1 to C_8 aliphatic hydrocarbons and aromatic

vapors of benzene, toluene and xylene, of which the major constituents were C_4 to C_6 alkanes. The total concentration of butane, pentane and hexane varied from 16 to 24 volume percent. Remaining hydrocarbons contributed to only about 1 volume percent.

Three different kinds of membranes have been experimented with: Celgard X-10 microporous polypropylene hollow fiber having a plasma polymerized nonporous silicone coating, a similar nonporous membrane based on a porous polypropylene substrate from Mitsubishi and ILMs (Immobilized Liquid Membranes) using both these membranes. ILMs are usually used in permeation studies to provide higher selectivities.

CHAPTER 2

THEORY AND MODELING OF PERMEATION/ SEPARATION OF HYDROCARBONS BY POLYMER MEMBRANES

2.1 Theory

2.1.1 Introduction

Membrane-based separation processes are, in general, driven by only three forces: gradients of concentration or partial pressure (gas, vapor and organic liquid permeation, dialysis), pressure (microfiltration, ultrafiltration and reverse osmosis) and electrical potential (electrodialysis). Permeance is the rate of transport of permeant species across the membrane per unit area per unit driving force, while selectivity is the relative rate of permeation of two different species per unit driving force of each species. These two characteristics of a membrane primarily characterize the performance of a membrane separation process.

Although membrane gas separation has been studied for over twenty years, vapor permeation was not given enough emphasis until recently. Pervaporation, a process analogous to vapor permeation, is used to treat liquid mixtures. The component to be separated permeates through the membrane into the gas phase on the permeate side which is generally maintained under vacuum. Applications of the membrane vapor separation process, like recovery of halogenated carbon compounds (chlorofluorocarbons (CFCs), hydrochlorofluorocarbons (HCFCs)) from industrial vent streams and retrieval of vinyl chloride monomer from PVC manufacturing process have already been commercialised in the United States. A number of membrane plants have been installed for recovery of

8

gasoline-derived hydrocarbon vapors from air streams, but only in Europe and Japan (Baker and Wijmans, 1994). This has been viewed with great economic importance for the past few years.

2.1.2 Theory of Permeation

The model used to predict membrane vapor permeation is the solution-diffusion model. According to this model, molecules of the vapor in the high-pressure side of the nonporous membrane (where the partial pressure is also higher), get dissolved in the membrane material, diffuse down a concentration gradient to the low-pressure side where they finally get desorbed. Two basic assumptions have been made; the vapor phases on either side are in thermodynamic equilibrium with their respective polymeric interfaces and sorption and desorption at these interfaces occur very rapidly compared to diffusion through the membrane. For preferential permeation through the membrane, the rate of permeation depends on the partial pressure difference on the two sides of the membrane (Wijmans and Helm, 1989), the membrane thickness and the permeability of that specific component. By definition, permeability of a species (Q) is the product of the diffusivity of the gas/vapor (D) through the membrane and its solubility (S). S_A/S_B, the ratio of the Henry's law sorption coefficients for species A and B respectively is termed the sorption (or solubility) selectivity and D_A/D_B, the ratio of the diffusion coefficients, is viewed as the diffusion selectivity. The quantity frequently measured from experiments is the ratio of the species permeability to the membrane thickness (δ_c), called permeance (Q/δ_c). It is easier to work with this quantity to avoid ambiguities in the values of the membrane thickness.

The permeability of small molecules like He or H_2 is high in polymeric membranes because of their high diffusivity whereas larger molecules like CO_2 also have higher permeabilities due to their high solubility in the membrane. Vapors, on the other hand, have significantly higher permeabilities because of their high condensibility and solubility. In all polymer materials, the diffusion coefficient decreases with increasing molecular size, because larger molecules interact more with the polymer chains than smaller molecules. Solubility, rather than diffusivity, of the organics in the polymer membrane determines the rate of transport of the organic molecules. High vapor pressures of the permeant species lead to higher diffusivities, hence resulting in higher permeabilities. Such a trend has been clearly observed for all organic vapors. Simple gases like N_2, O_2 etc. do not follow this trend since their permeabilities are not a function of their gas phase partial pressure. Nonporous rubbery silicone membranes are widely used for vapor separation (Peinemann et al., 1986) since they have extremely high permeances for VOCs and lower permeances for nitrogen or oxygen.

2.1.3 Form and Structure of Vapor Permeation Membranes

Hollow fiber membranes are self-supporting against any applied pressure difference while flat membranes need additional mechanical support. Vapor permeation is almost exclusively performed with thin film composite (TFC) membranes consisting of an ultrathin, selective, nonporous, rubbery top layer backed by an unselective porous/ microporous support. The particular Celgard X-10 fibers, the hollow fiber membranes used in this study, have an ultrathin silicone coating on the outside. The Celgard X-10 polypropylene substrate (Hoechst Celanese, Charlotte, NC) has a porosity of 0.3. The

coating performs the separation while the porous support provides mechanical strength. It is desirable that the substrate material is cheap and offer reasonably good resistance to solvents. Polypropylene meets these requirements better compared to polysulfone and polyimide (Strathmann et al., 1986; Kimmerle et al., 1988).

Hollow fibers used for experimental purposes have been obtained from AMT (Applied Membrane Technology, Minnetonka, MN). These fibers (ID/OD: 240/290 μm) have a very thin coating ($\sim$ 1 μm) of silicone deposited through plasma polymerization on the outside surface of the basic microporous polypropylene substrate (Celgard X-10). The plasma-polymerized layer could withstand a pressure difference of 200 psia (Papadopoulos, 1992). Commercial availability is another important aspect that has been considered before deciding to use these membranes. Hollow fiber modules were fabricated in the laboratory using these membranes. This has been described in detail in Chapter 3.2. Two other kinds of composite membranes, one with a silicone fluoropolymer coating and another with a silicone hydrocarbon coating were also used for experiments. In both cases, the substrate was microporous polypropylene (KPF 205, Mitsubishi).

2.1.4 Immobilization of Liquid in the Fiber Pores

An unique and innovative aspect of this investigation is the attempt made to study the vapor separation behavior of an immobilized liquid membrane. Immobilization is the process of filling the pores of the polymer (substrate) matrix with an inert liquid which would offer more resistance to the passage of nitrogen than to that of other organics. It enhances the separation efficiency of the overall composite membrane since the

immobilized liquid in the membrane pores acts as another permselective layer in addition to the selective silicone coating. The hydrophobic supports are chemically inert allowing immobilization of a variety of aqueous and organic liquids. There is practically no swelling as a result of liquid immobilization in these hydrophobic supports though this phenomenon has been observed for hydrophilic films. Immobilized liquid membranes (ILM) with polyethylene glycol in pores have been used for CO_2-O_2 separation (Ward et al., 1967) and for removal of H_2S from gasified coal (Matson et al., 1977).

Since the pressure needed to expel the liquid from the membrane pores is inversely proportional to the radius of the pore for a system with given interfacial tension, higher pressures of operation can be achieved with finer pores in the support membrane. One problem involves reducing the film thickness from around 45 μm to lower levels (approximately 5 μm) to obtain higher flux values (Bhave and Sirkar, 1986), but this also requires that the support film porosity be high and tortuosity be low, to capitalize on low film thickness. In this study, efforts were made to immobilize liquids in both membranes, one being the Celgard X-10 substrate, the other being Mitsubishi KPF 205 substrate. Figure 1 shows the transport mechanism in ILM.

2.2 Mathematical Model

2.2.1 Equations

A mathematical model has been developed to simulate the experimental results under the operating conditions. One of the primary objectives of such a model would be to illustrate the difference, if any, between passing the feed on the tube side and on the shell side. Another unique aspect of this model is the attempt made to incorporate substrate

Feed Gas Flow →

Permeate

Vacuum

Silicone Coating

Microporous Substrate

Liquid (PEG/PEGDE) Immobilized in Substrate Pores

Vacuum
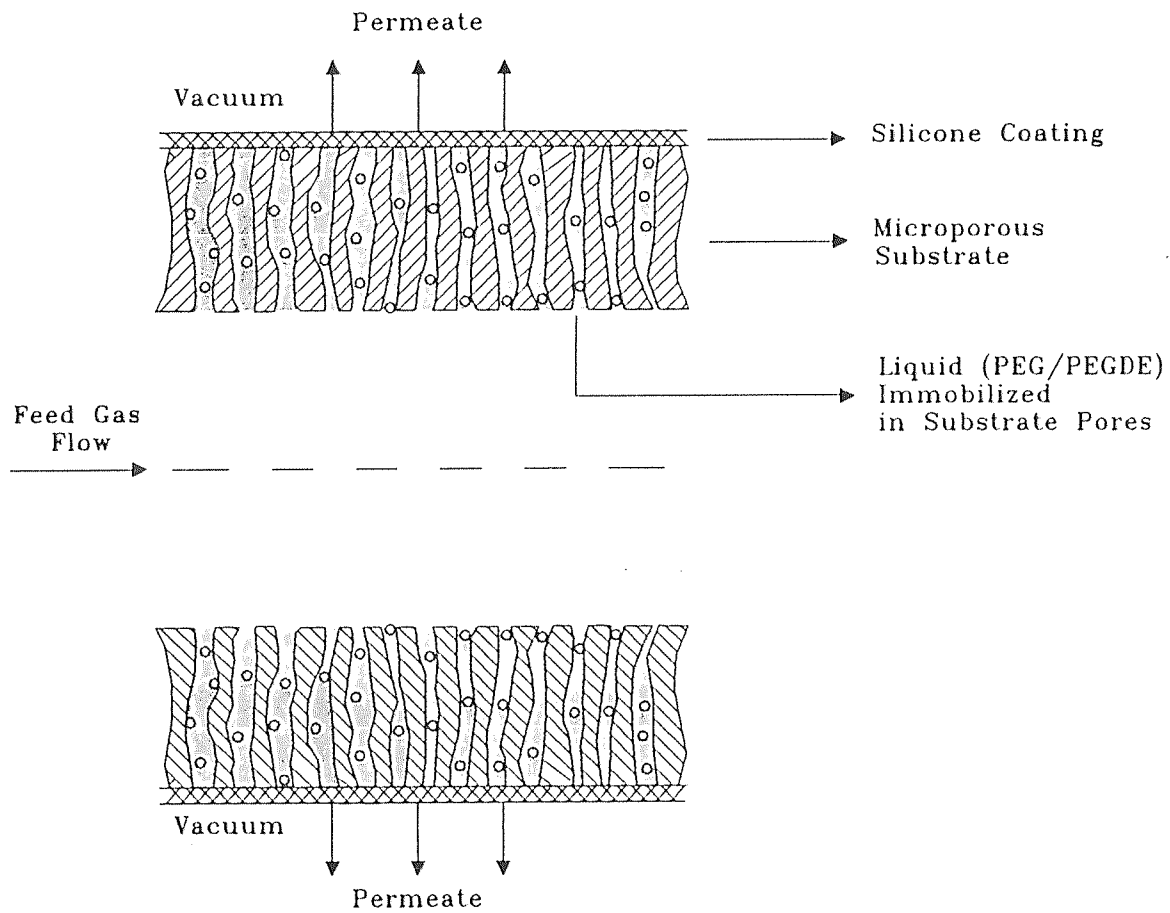
Permeate

Figure 1. Mechanism of Transport in Immobilized Liquid Membrane

pressure drop in the shell side feed mode (refer to Figure 2).

Driving force for permeation is the gradient of partial pressure difference. Low pressure on the permeate side is maintained by means of a vacuum pump. The hollow fibers are actually composite membranes i.e. an ultrathin coating (~ 1-2 μm) of polydimethylsiloxane (PDMS, also called silicone) is deposited through plasma polymerization on the surface of these polypropylene hollow fibers. Consequently, when feed is passed from one side, the permeating molecules encounter two different resistances; one due to the coating and the other due to the substrate.

The equations are as described in the following pages. Since, the case of simple permeation is a steady state process, the equations are time-independent and the segmental permeation equations involve solving four linear equations for four basic unknown variables.

For modeling purposes, the entire length of the module has been divided into a fixed number of small segments. A typical permeating segment based on which these flux equations have been developed along with flow directions of the vapor, is shown in Figures 3 and 4. Figure 3 also shows the direction of permeate flow in both, cocurrent and countercurrent modes of separation.

Permeation across skin for component 1:

$$N_1 = \frac{Q_1}{\delta_c} [P_f x_f - (p' y_1) \mid_{z \to s}]$$

(1)
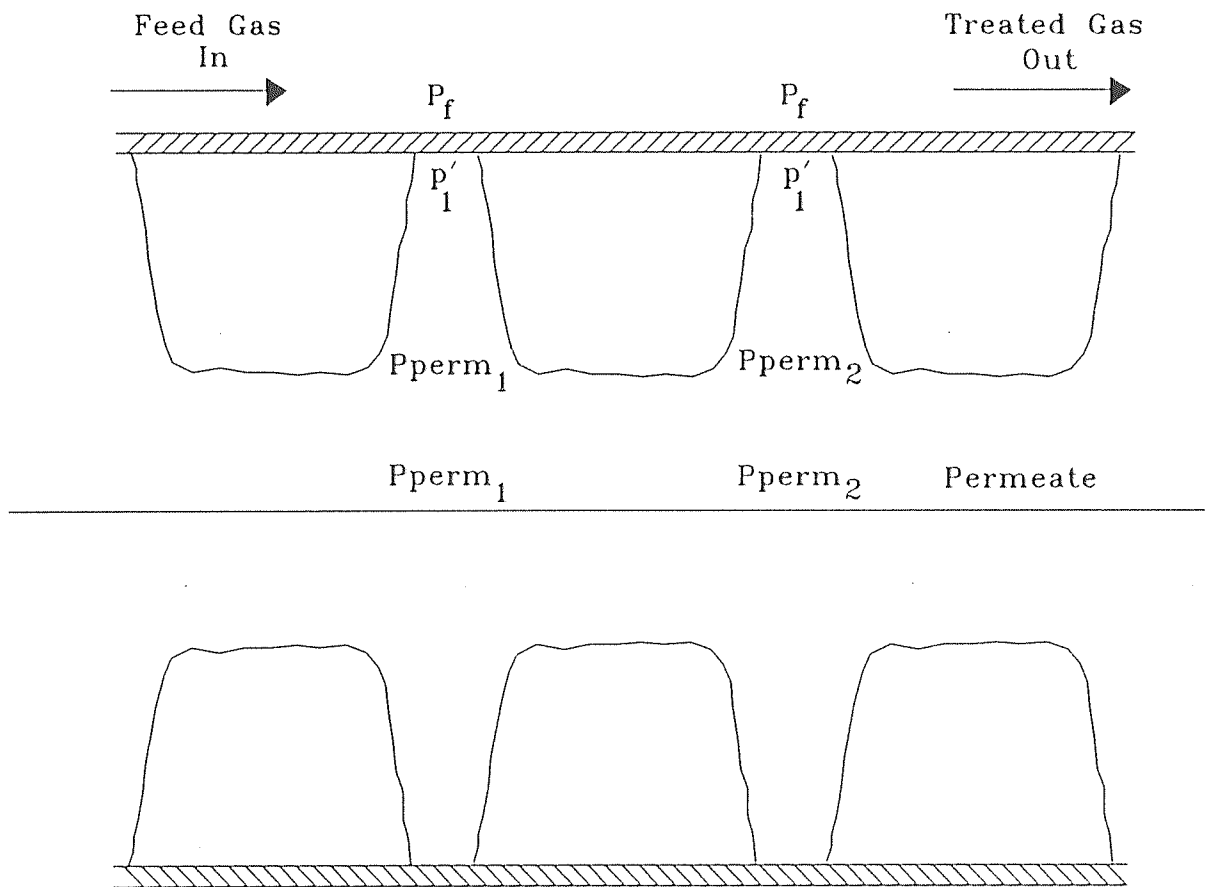
Figure 2. Illustration of Pressure Drop in Substrate Pores

HC laden
Stream
(FEED)

HC lean
Stream
(RETENTATE)

Silicone Skin

Microporous
Polypropylene
Substrate

Countercurrent Mode
Permeate Flow

HC-rich
Stream
(PERMEATE)

Cocurrent Mode
Permeate Flow
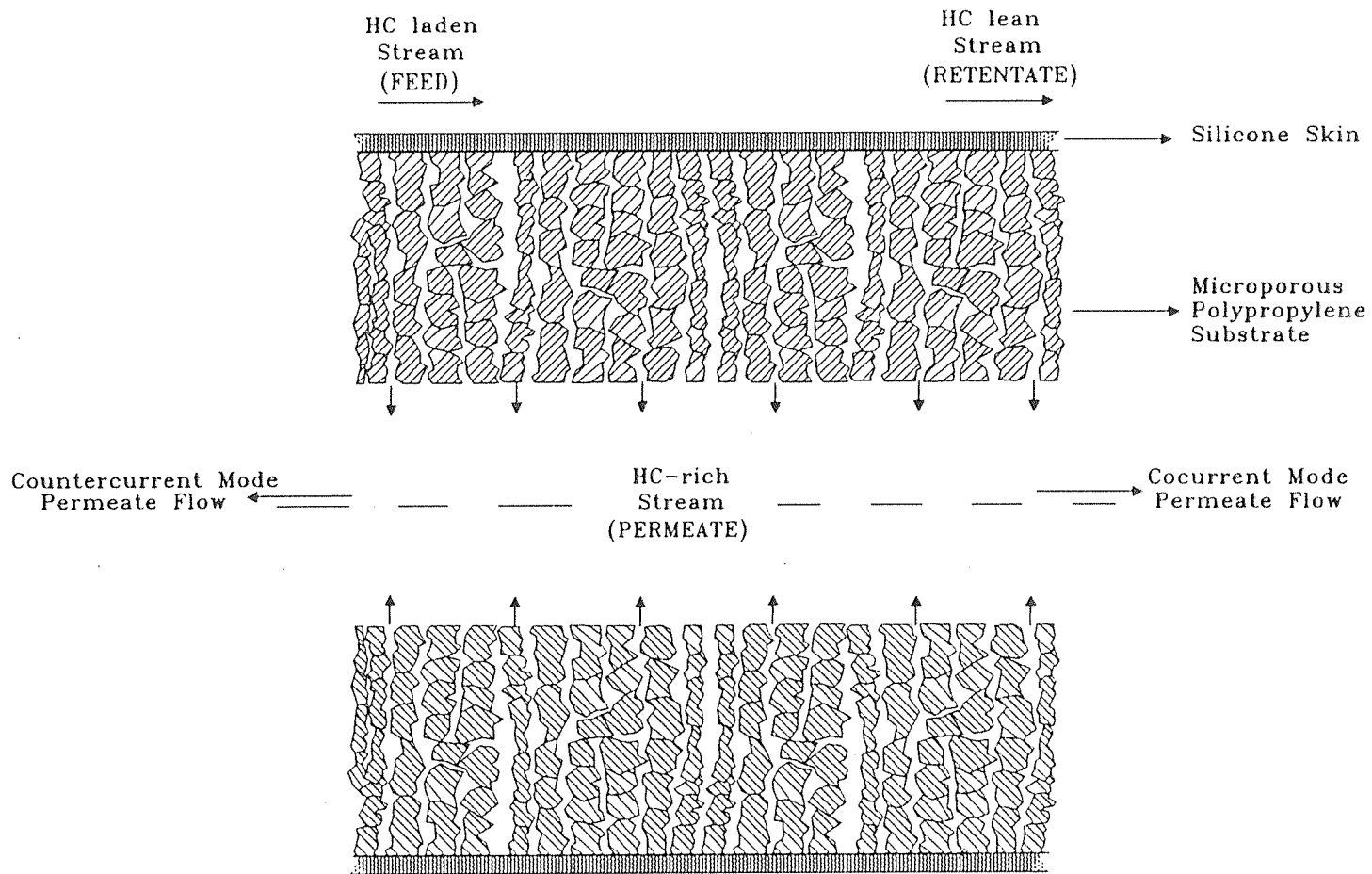
Figure 3. Flow Directions in a Segment

$$(X_{in} = X_f)$$

$P_f \quad L_{in} X_{in}$ $\mid$ ithsegment $\mid$ $P_f \quad L_{out} X_{out}$

$P_f \quad X_f$

$Z = \delta + \delta_c$

$Z = \delta$

$p' \quad y_1$

$Z = 0$

Permf(i)

$V_{out} Y_{out}$
PPERM

Permf(i+1)

$P_f \quad L_{in} X_{in}$ $\mid$ $\mid$ $P_f \quad L_{out} X_{out}$

Figure 4. Mole Balance in a Segment

Permeation across skin for component 2:

$$N_2 = \frac{Q_2}{\delta_c} [P_f(1-x_f) - (p^-(1-y_1)) \mid_{z=\delta}] \tag{2}$$

Knudsen diffusion equation for component 1 in porous substrate:

$$N_1 = \frac{D_{k1}}{RT\delta} [(p^- y_1) \mid_{z=\delta} - (p^- y_1) \mid_{z=0}] \tag{3}$$

Knudsen diffusion equation for component 2 in porous substrate:

$$N_2 = \frac{D_{k2}}{RT\delta} [(p^-(1-y_1)) \mid_{z=\delta} - (p^-(1-y_1)) \mid_{z=0}] \tag{4}$$

Cross flow condition at $z=\delta$:

$$\frac{y_1 \mid_{z=\delta}}{1-y_1 \mid_{z=\delta}} = \frac{N_1}{N_2} = \frac{\frac{Q_1}{\delta} [P_f x_f - (p^- y_1) \mid_{z=\delta}]}{\frac{Q_2}{\delta} [P_f(1-x_f) - (p^-(1-y_1)) \mid_{z=\delta}]} \tag{5}$$

Adding equations (3) and (4)

$$p^- \big|_{z=\delta} - p^- \big|_{z=0} = \frac{N_1 \delta RT}{D_{k1}} + \frac{N_2 \delta RT}{D_{k2}} \qquad (6)$$

Adding equations (1) and (2)

$$P_f - p^- \big|_{z=\delta} = \frac{N_1 \delta_c}{Q_1} + \frac{N_2 \delta_c}{Q_2} \qquad (7)$$

Adding equations (6) and (7)

$$P_f - p^- \big|_{z=0} = N_1 \left[\frac{\delta RT}{D_{k1}} + \frac{\delta_c}{Q_1} \right] + N_2 \left[\frac{\delta RT}{D_{k2}} + \frac{\delta_c}{Q_2} \right] \qquad (8)$$

Rewriting equations (1) and (3)

$$N_1 \frac{\delta_c}{Q_1} = P_f X_f - (p^- Y_1) \big|_{z=\delta} \qquad (9)$$

$$N_1 \frac{RT\delta}{D_{k1}} = (p^- Y_1) \big|_{z=\delta} - (p^- Y_1) \big|_{z=0} \qquad (10)$$

Adding (9) and (10)

$$N_1 [\frac{\delta_c}{Q_1} + \frac{\delta RT}{D_{k1}}] = P_f x_f - (p^- y_1)\,|_{z=0} \tag{11}$$

Rewriting equations (2) and (4)

$$N_2 \frac{\delta_c}{Q_2} = P_f(1-x_f) - (p^-(1-y_1))\,|_{z=\delta} \tag{12}$$

$$N_2 \frac{RT\delta}{D_{k2}} = (p^-(1-y_1))\,|_{z=\delta} - (p^-(1-y_1))\,|_{z=0} \tag{13}$$

Adding (12) and (13)

$$N_2 [\frac{\delta_c}{Q_2} + \frac{\delta RT}{D_{k2}}] = P_f(1-x_f) - (p^-(1-y_1))\,|_{z=0} \tag{14}$$

Equation (8) could also be obtained by adding equations (11) and (14). Lumped resistances in equation (8) can be replaced by overall resistances $1/\alpha$ and $1/\beta$ for components 1 and 2, respectively.

$$\frac{1}{\alpha} = \frac{1}{\dfrac{D_{k1}}{\delta RT}} + \frac{1}{\dfrac{Q_1}{\delta_c}} \qquad (15)$$

$$\frac{1}{\beta} = \frac{1}{\dfrac{D_{k2}}{\delta RT}} + \frac{1}{\dfrac{Q_2}{\delta_c}} \qquad (16)$$

Equation (8) can now be written as

$$P_f - p' \big|_{z=0} = \frac{N_1}{\alpha} + \frac{N_2}{\beta} \qquad (17)$$

where α and β are permeances measured from experiment. Equations 1, 2, 5 and 9 have to be solved simultaneously for unknowns $p'|_{z=\delta}$, $y_1|_{z=\delta}$, N_1 and N_2 . This is the methodology adopted for one segment.

$$N_1 = \alpha \left[P_f x_f - (p' y_1) \big|_{z=0} \right] \qquad (18)$$

$$N_2 = \beta \left[P_f (1 - x_f) - (p'(1 - y_1)) \big|_{z=0} \right] \qquad (19)$$

Generally

$$\frac{1}{overall\ permeance} = \frac{1}{Knudsen\ permeance} + \frac{1}{skin\ permeance} \qquad (20)$$

Performing mole balance for the segment under consideration (refer to Figure 4)

$$V_{out}(i) = (N_1 + N_2)\Delta A \qquad (21)$$

$$L_{out}(i) = L_{in}(i) - V_{out}(i) \qquad (22)$$

$L_{in}(i)$, $X_{in}(i)$ and P_f are known.

$$Y_{out}(i) \approx y_1|_{z=0} = \frac{(p^- Y_1)|_{z=\delta} - N_1 \frac{\delta RT}{D_{kl}}}{p^-|_{z=0}} \qquad (23)$$

$$X_{out}(i) = \frac{L_{in}(i)X_{in}(i) - V_{out}(i)Y_{out}(i)}{L_{out}(i)} \qquad (24)$$

In the countercurrent mode

$$Permf(i) = V_{out}(i) + Permf(i+1) \tag{25}$$

But the permeate pressures in each successive segment are related by the Hagen-Poiseuille equation for compressible flow (Pan and Habgood, 1978) to the permeate flow rate from each segment.

Permeate pressure in segment i: Pperm(i)

Permeate flow rate from segment i: Permf(i)

Length of the module: L

$$[Pperm(i+1)]^2 - [Pperm(i)]^2 = \frac{256\mu RT\Delta L}{\pi d_i^4} Permf(i) \tag{26}$$

Starting from segment i=1 at axial location l=0, a guess value for permeate flow rate (from segment i=1) is used for the first segment. An appropriate guess could be the difference between the inlet and outlet flow rates measured from the experiment. Once, the set of four equations is solved for segment i=1, $V_{out}(i)$ is also known. Permf(i+1) can be calculated from equation (25). Pperm(i+1) can be calculated from (26). The above set of calculations is repeated iteratively for segments i=1 to 100, until axial location l=L is reached.

However, in the vacuum mode of operation, one end of the module is usually sealed. For the last segment, the value of permeate $V_{out}(100)$ should match the value of

permeate flow rate Permf(100). An error criterion could be set for the tolerance of this value. If the value of error exceeds this limit, the guess value of permeate flow rate is adjusted to the new calculated value and the set of calculations is repeated until convergence. The results of this mathematical model and comparison of these results with experimental data are discussed in Chapter 4.2.

CHAPTER 3

EXPERIMENTAL PROCEDURE FOR REMOVAL OF HYDROCARBONS

3.1 Approach

To achieve the objectives mentioned in Chapters 1 and 2, experiments were carried out with different hollow fiber modules consisting of different kinds of membranes. A gas mixture consisting of 12% butane, 4% pentane, 1% hexane, 83% nitrogen was usually used as the feed, although, in some cases this mixture was diluted with nitrogen. Following sections describe the general procedure and materials used for the experimental work.

3.2 Hollow Fiber Module Fabrication

Two identical modules were fabricated in house using the hollow fiber membranes supplied by AMT (Minnetonka, MN). Two other modules were also procured as such from AMT Inc. These fibers are thin film composite membranes. An ultrathin layer of silicone rubber (membrane) is coated on the surface of a porous polypropylene (substrate) hollow fiber via a plasma polymerization process. Fibers were taken from the roll and cut to a length, little longer than the 1/4" stainless steel tubing used as the module shell. The stainless steel tubing was fitted with 1/4" male run tees at both ends. The required number of fibers were matted on a vinyl sheet on a table. Deionized water was sprayed on these hydrophobic coated fibers for ease of handling. The fibers laid out were bundled

and one end was tied with a string. This end was pulled through the bore of the stainless steel tubing.

A leak-free tube sheet was prepared at the two ends of the tubing to serve two purposes. The tube sheet held the bundle of fibers in place and prevented the shell side and tube side fluids from mixing. A three-layer potting was done to prepare a tube sheet for the module. Figure 5 shows the details of potting. A two component RTV118 translucent silicone rubber adhesive sealant (General Electric Co., Waterford, NY) was applied as the first layer at the end of the fiber bundle. This material is very suitable for potting the first layer due to its viscous nature and good compatibility with the silicone fibers. After curing for one day, another two component silicone rubber, RTV615 (General Electric Co., Waterford, NY) was prepared by mixing 10% by weight of curing agent (B) with the silicone compound (A). The mixture was placed in a desiccator and gases resulting from the addition-hydrosililation reaction were removed using a vacuum pump and were vented through a hood. After curing for a week, epoxy (C-4: resin, D: activator, weight ratio: 4/1; Beacon Chemicals, Mt.Vernon, NY) was applied as the third layer through the shell side using a glass dropper. Epoxy was used as the third layer because the sealing properties with metal parts are better than those of silicone rubber adhesive which had very good bonding with the fiber. In retrospect, one layer of potting adheres to the fibers and this layer, in turn, binds to the inside of the tubing via the epoxy layer. Both ends of the module were potted this way. The effective module length would be the length of the stainless steel tubing less double the potting thickness (to account for both sides of the potting).

Figure 5. Three Layer Potting
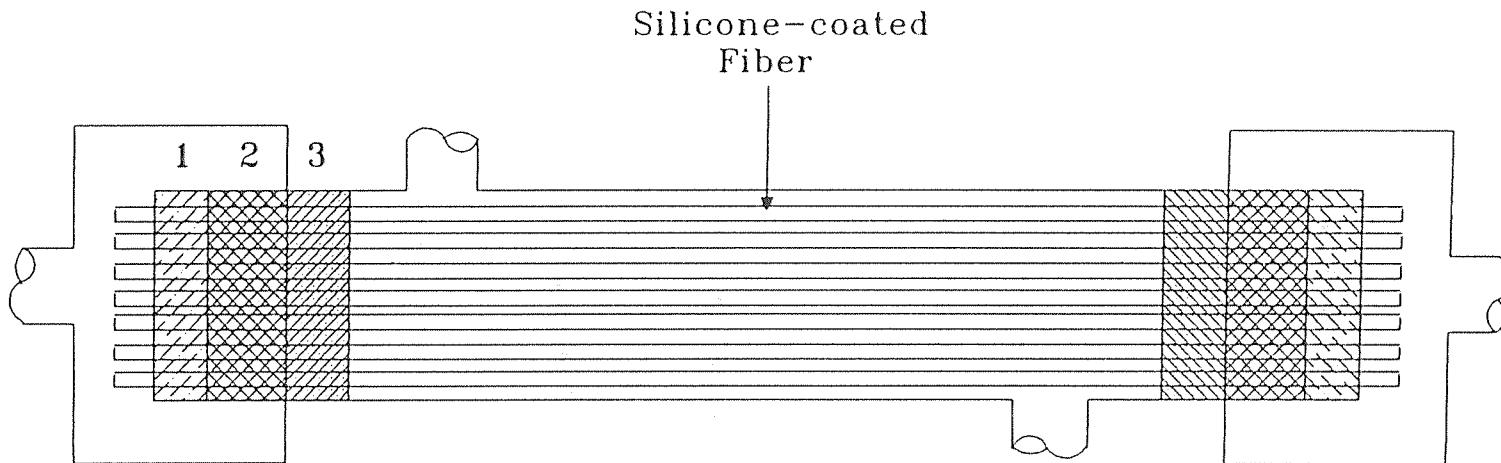
1 st layer: Silicone rubber RTV118 A & B
2 nd layer: Silicone rubber RTV615 A & B
3 rd layer: Epoxy C-4 & D

3.3 Module Testing and Measurement of Nitrogen Permeation

Specifications of modules used for these experiments are provided in Table 1. Before using these modules for vapor permeation studies, some preliminary tests were carried out. For testing leakage, the shell side of the module was filled with deionized water. Water pressure was maintained at 15-20 psi for about 2-3 hours. If no water leaked through the potting, the module was considered leak-free. Pure nitrogen was passed through the tube side and the shell side for couple of hours to completely dry these hydrophobic fibers. Typical setup used for leak-testing is shown in Figure 6.

An estimate of nitrogen permeation is also very essential to select operating feed flow rates for the permeation process. Figure 7 shows the schematic of the setup for nitrogen permeation studies.

3.4 Experimental Setup for Removal of Hydrocarbons from Nitrogen

3.4.1 Materials, Chemicals and Equipment

The materials, chemicals and equipment used for experiments are listed below:

Multiple Flow Controller (Model 8274, Matheson, East Rutherford, NJ)

Mass Flow Transducer (Model 8272-0422, Matheson, East Rutherford, NJ)

Mass Flow Transducer (Model 8272-0412, Matheson, East Rutherford, NJ)

Silicone-Coated Hollow Fibers (AMT, Minnetonka, MN)

Gas Chromatograph (GC, Hewlett Packard Model 5890A)

Automatic 6-port Gas Sampler (Hewlett Packard)

Automatic 10-port Gas Sampler (Hewlett Packard)

Dual Channel Integrator (Hewlett Packard Model 3392A, Series III)

Table 1. Specifications of Modules Used for Gasoline Vapor Permeation

Module	Membrane Support	Membrane Coating	No. of Fibers	ID/OD (μm)	Active Length (cm)	Active Surface Area (cm^2)
EPA/GVP-1*	Celgard X-10	Silicone	50	240/290	25.4	115.7
EPA/GVP-2	KPF 205 Mitsubishi	Silicone Fluoropolymer	71	205/255	23.5	107.4
EPA/GVP-3	KPF 205 Mitsubishi	Silicone Hydrocarbon	71	205/255	23.5	107.4
EPA/GVP-4*	Celgard X-10	Silicone	50	240/290	25.4	115.7
EPA/GVP-5*	Celgard X-10	Silicone	50	240/290	12.7	57.85
EPA/GVP-6*	Celgard X-10	Silicone	15	240/290	6.0	8.19

* Fabricated in house. 1, 4, 5 and 6 use later versions of AMT membrane

PR

HF

CE

N₂

PV   HFM

TLP
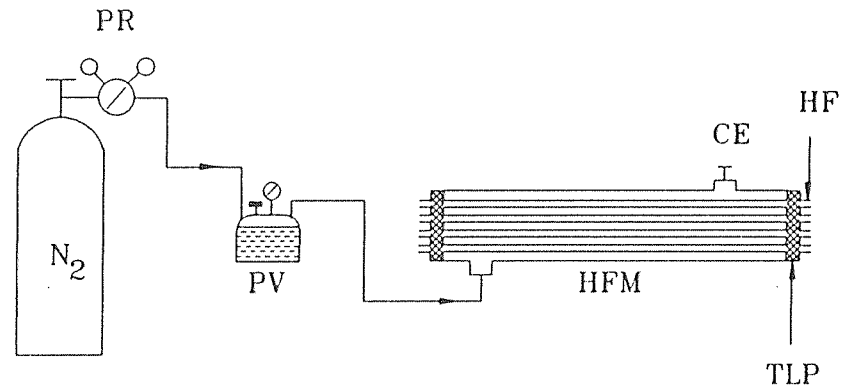
N₂ : High Purity Nitrogen Gas Cylinder

PR : Dual Stage Pressure Regulator

PV : Pressure Vessel (filled with water)

HFM : Hollow Fiber Module

CE : Closed End

HF : Hollow Fiber

TLP : Three Layer Potting

Figure 6. Setup for Leak-testing Hollow Fiber Modules
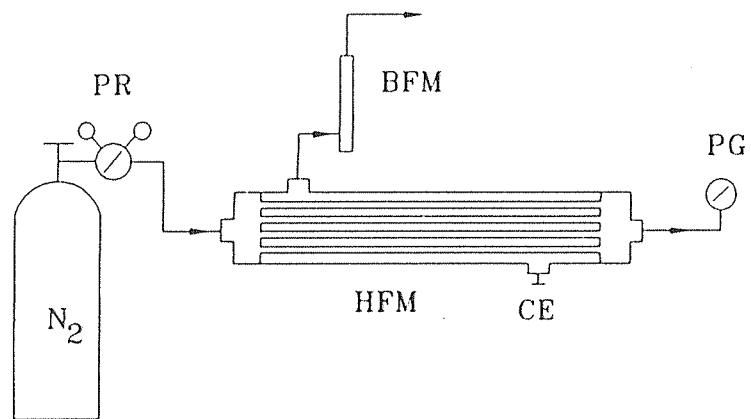
PR : Dual Stage Pressure Regulator
N$_2$: High Purity Nitrogen Gas Cylinder
HFM : Hollow Fiber Module
BFM : Bubble Flow Meter
CE : Closed End
PG : Pressure Gauge

Figure 7. Setup for Measurement of Nitrogen Permeation

Vacuum Pump (Model UN 726.1.2.FTP, KNF Neuberger Inc., Trenton, NJ)

Vacuum Gauge (Heise, Newtown, CT)

Double Chamber Vacuum Trap (Aldrich Chemical Co., Milwaukee, WI)

Bubble Flow Meter (Varian, Sugarland, TX)

Pressure Gauges (Model 63-5631, Matheson, East Rutherford, NJ)

Constant Temperature Bath Heater (Haake, Germany)

Nitrogen Dry, Nitrogen Zero, Hydrogen Zero, Helium Zero, Air Zero, Gasoline Mixture (Butane:12%, Pentane:4%, Hexane:1%, Nitrogen: 83%), Butane:120000 ppmv, Pentane:40000 ppmv, Hexane:10000 ppmv (Matheson, East Rutherford, NJ)

Liquid n-Pentane, Liquid n-Hexane (Aldrich Chemical Co., Milwaukee, WI).

3.4.2 Experimental Procedure

Experiments were carried out in a setup (Figure 8) in which all connecting lines were ⅛" or ¼" S.S.tubing. Fittings (unions, tees, valves etc.) of both sizes were procured from R.S.Crum (Mountainside, NJ). Feed gas was supplied directly from a primary standard gas mixture cylinder (Matheson, E.Rutherford, NJ) or prepared by blending this standard gas mixture with pure nitrogen. Desired feed compositions were obtained by blending the hydrocarbon mixture of known composition with pure nitrogen in appropriate ratios. Gas flow rates were controlled by electronic mass flowmeter-controllers (Matheson, E.Rutherford, NJ) and measured by a bubble flow meter. Driving force for permeation i.e. gradient of partial pressure difference for each component, was created by applying a vacuum on the permeate side.

FT: Flow Transducer
FC: Flow Controller
TWV: Three Way Valve
SP: Sampling Port
PG: Pressure Gauge
HFM: Hollow Fiber Module
VG: Vacuum Gauge
VP: Vacuum Pump
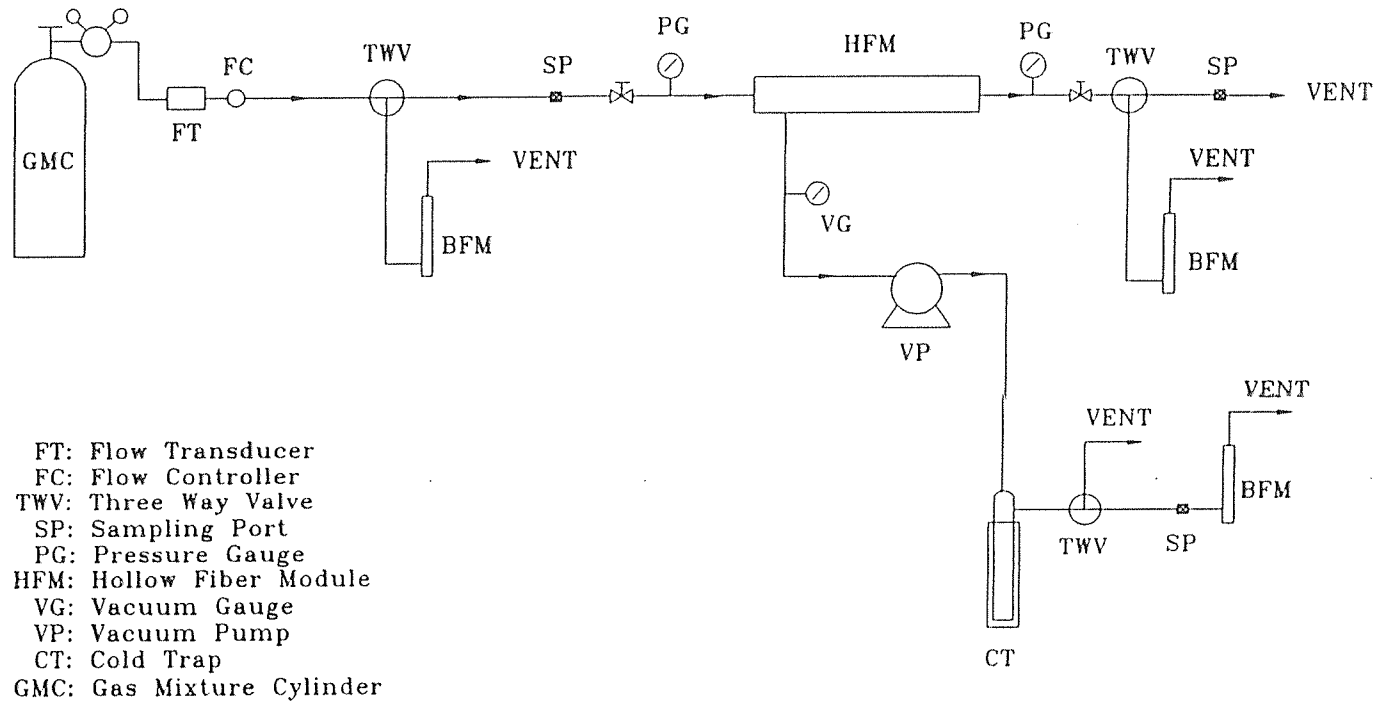CT: Cold Trap
GMC: Gas Mixture Cylinder

Figure 8. Experimental Setup for Gasoline Vapor Permeation

The lines were connected in such a way that a sample of the feed gas as well as the treated retentate gas could be sent to a gas chromatograph (GC) for analysis. Needle valves were used to control these sample flow rates at about 2 cc/min. Use of three-way switching valves in the inlet and outlet lines enabled intermittent measurement of respective flow rates. For the treated gas, however, rest of the flow was vented. Concentrations of individual components in the feed and retentate streams could either be ascertained from the GC calibration plots prepared for each component or determined from the ratio of respective peak areas of the inlet and the outlet streams when concentration of the inlet stream is known. Analysis of the permeate was relatively difficult because of the inability to install 100% leak-proof vacuum connections. Vapor condensation inside the lines was another probable factor compounding the difficulty of analysis.

Inlet and outlet pressures of the gas were monitored through pressure gauges (Matheson, E.Rutherford, NJ). A lower pressure on the permeate side (1-2 cm Hg) was maintained by a vacuum pump (KNF Neuberger, Trenton, NJ). Permeate pressure was monitored through a vacuum gauge (Heise, Newtown, CT) and could be controlled at the desired level by adjusting a valve manually. After each experimental run, nitrogen ($\sim$ 10 cc/min) was passed through the module overnight, to remove any trace of organics that may be present.

Experiments to study separation behavior of individual components were also done with binary mixtures (i.e. hydrocarbon and nitrogen). Butane, pentane and hexane were the three hydrocarbons of interest. The setup described above was retained for these experiments.

In this study, experiments were done, both with feed on the tube side and vacuum on the shell side and vice versa. Keeping the shell side end adjoining the retentate end closed, ensured countercurrent mode of operation which would result in better separation because of a higher partial pressure difference than the cocurrent mode. This is analogous to higher efficiency in the countercurrent heat exchange process in a shell-and-tube heat exchanger.

3.4.3 Experiments with Reduced Vacuum

In industrial practice, vacuum levels are usually lower than the levels (1-2 cm Hg) used in laboratory experiments. To study the effect that higher permeate pressure (i.e. reduced vacuum level) may have on the separation behavior, experiments were done maintaining permeate pressure at 5 cm Hg. This was done by incorporating a control valve which could be adjusted manually until a desired vacuum level reading was obtained on the gauge.

3.4.4 Immobilization of Liquids in Substrate Pores

For immobilizing liquids in the polypropylene substrate pores, inert liquids like polyethylene glycol (PEG) and polyethylene glycol dimethyl ether (PEGDE) were used. Attempts to wet a sample of the membrane with the pure liquid were unsuccessful. It was decided to dissolve PEG in a solvent that would wet the fiber and then immobilize the liquid in the membrane pores with this solution. The same procedure was followed for the other inert liquid viz. PEGDE. A typical solvent chosen for these purposes would be easily vaporizable. The following procedure was adopted for immobilization.

1. Dissolve PEG/PEGDE in ethanol in the volume ratio of 60:40. This ratio was found

to be optimum after conducting elementary wetting tests with a flat membrane.

2. Circulate the solution for about 3-4 hours through the tube side of the module.

3. Drain and purge with nitrogen to remove residual ethanol from the pores.

3.4.5 Introduction of Feed from the Shell Side

Permeation/ separation process was usually studied by introducing the feed on the tube

side and maintaining vacuum on the shell side of the module. Some experiments were

also carried out to observe the effect of introducing the feed on the shell side and

sustaining vacuum on the tube side. Identical conditions were ensured (such as flow rate,

concentration, feed pressure, permeate pressure) to obtain a better comparison of the

separation behavior of the membrane module in both modes of operation.

3.5 Analytical Measurement

A Hewlett-Packard 5890 series II gas chromatograph (Hewlett Packard, Wilmington, DE)

was used to ascertain the composition of both inlet and outlet streams. Hydrocarbons

were analyzed using a 60 m long capillary column (HP-1 cross-linked Methyl Silicone

Gum) obtained from Hewlett Packard (Wilmington, DE) and nitrogen was analyzed

using a 6 ft long packed column (molecular seive 13X, 60/80 mesh) procured from

Hewlett Packard. To quantitatively detect these separately, the capillary column was

connected to a Flame Ionization Detector (FID) and the packed column was connected

to a Thermal Conductivity Detector (TCD). The flow diagrams of the sample through

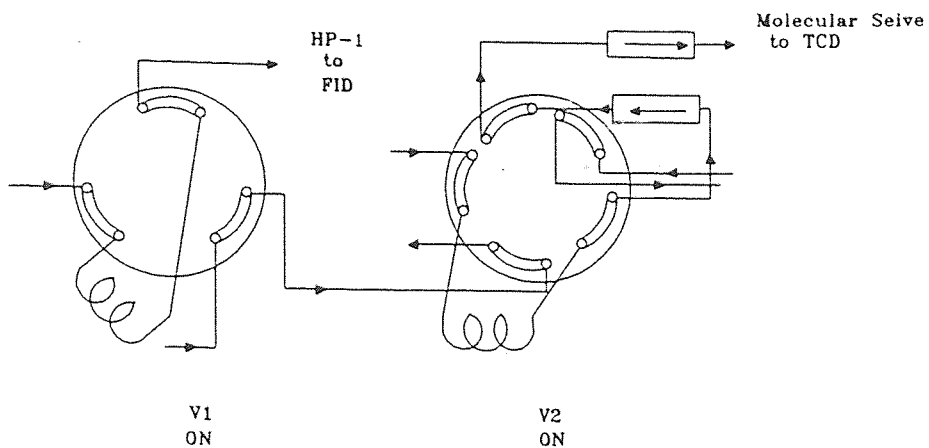the loop are shown in Figures 9 and 10 when the valves are either in the ON position or

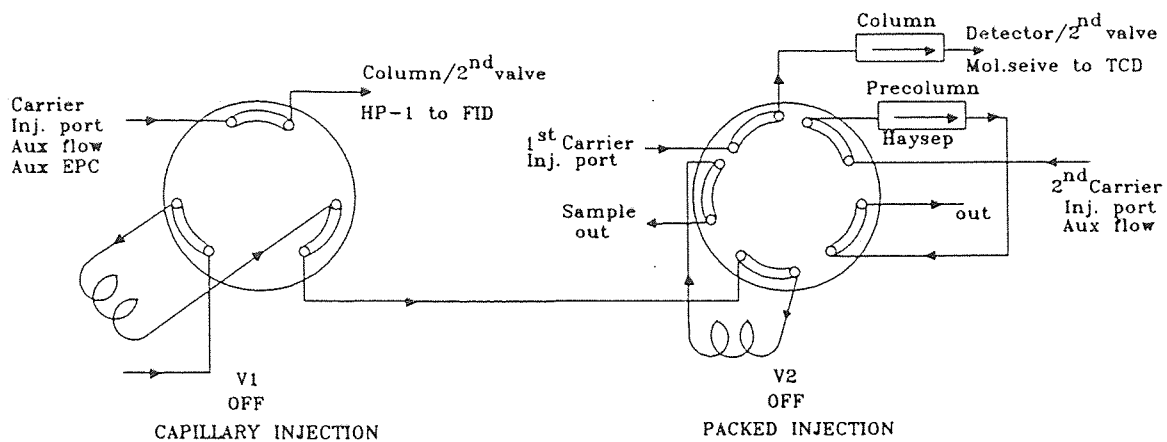**Figure 9.** Sample Flow Diagram in the ON Position

Figure 10. Sample Flow Diagram in the OFF Position

in the OFF position. Sample GC calibration curves for butane, pentane, hexane and nitrogen are shown in Figures 11, 12, 13 and 14.

3.6 Measurement of the Permeance of Hydrocarbons

The setup for permeance measurement (Figure 15) was very similar to the general experimental setup. Since the value of permeance measured has to be at a specific concentration, the difference in concentration between the inlet and the outlet streams (i.e. percent removal of these organics) had to be minimized. With this objective, experiments were done with a smaller module (module #6 in Table 1), whose length was about ⅓rd the length of the modules used for permeation-separation studies. Percent removal of individual components did not exceed 5-6%. Concentrations of individual hydrocarbons were manipulated by blending with appropriate proportions of nitrogen. Gas mixture cylinders containing 12% butane, 88% nitrogen or 4% pentane, 96% nitrogen or 1% hexane, 99% nitrogen were separately obtained from Matheson (E.Rutherford, NJ). These studies were performed at a flow rate of ~60 cc/min. Further permeance measurements were done using the model gasoline mixture (~12% butane, ~4% pentane, ~1% hexane, ~83% nitrogen) to observe the influence of competing permeating species.

$$Y = -794.79 + 6.375E\text{-}3*X - 3.869E\text{-}11*X^2$$
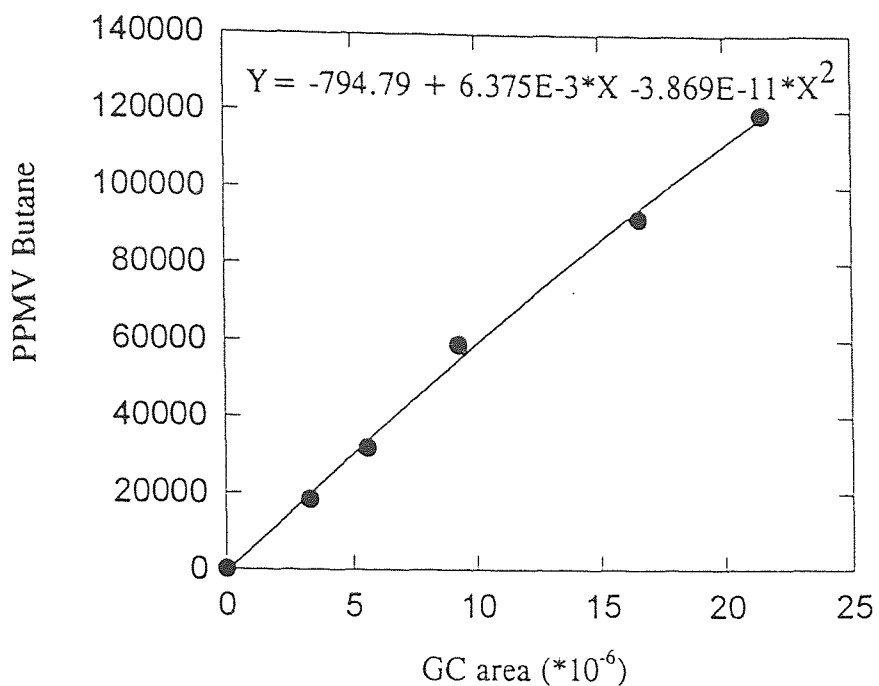
Figure 11. Gas Chromatograph Calibration Curve for Butane

$$Y = -274.8 + 5.0802E\text{-}3*X - 6.315e\text{-}11*X^2$$
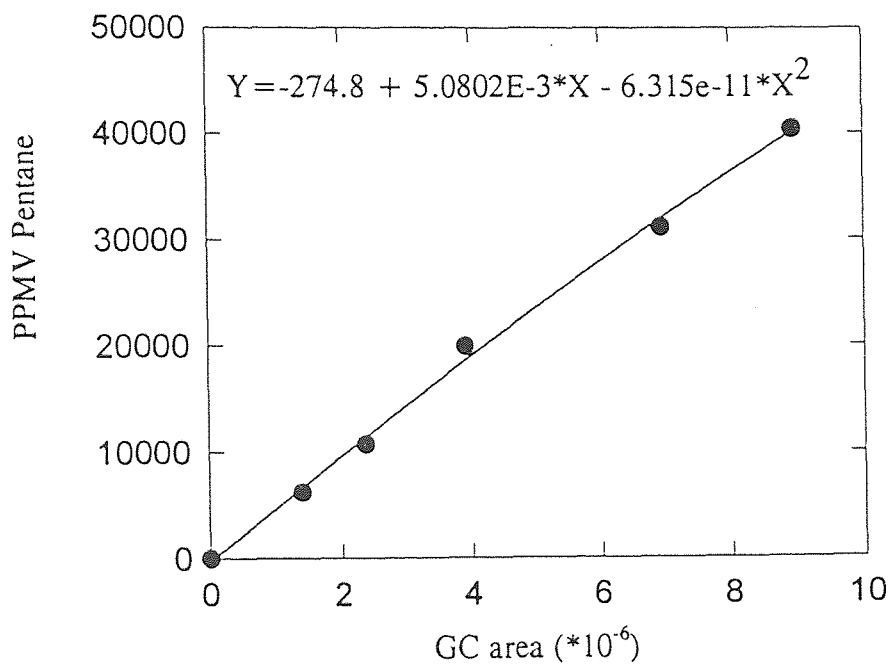
Figure 12. Typical Gas Chromatograph Calibration for Pentane
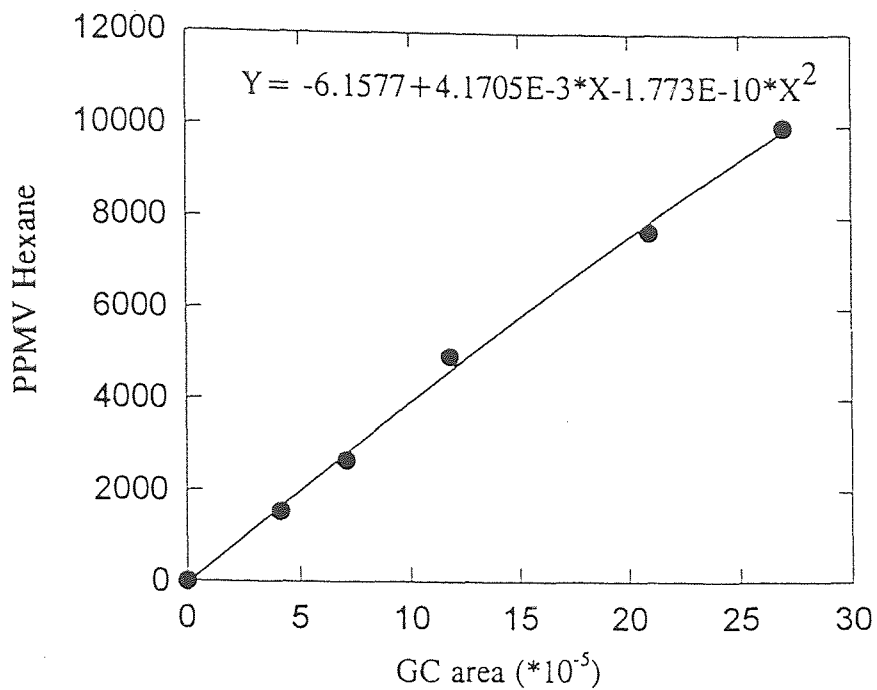
Figure 13. Typical Gas Chromatograph Calibration for Hexane

In the chart: $Y = -6.1577 + 4.1705E\text{-}3*X - 1.773E\text{-}10*X^2$
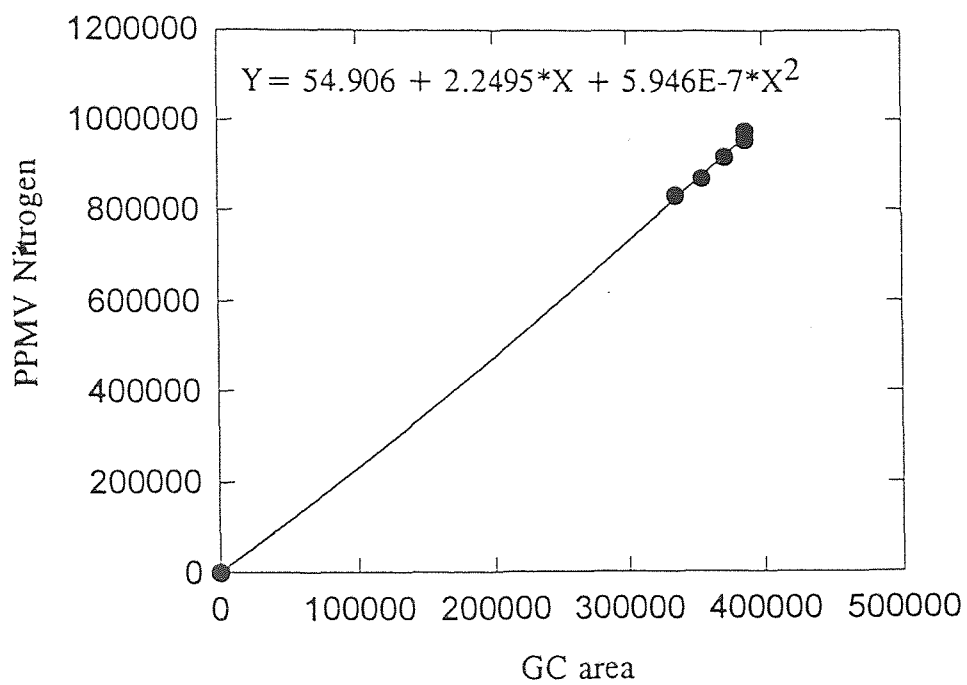
Figure 14. Sample Gas Chromatograph Calibration for Nitrogen

In the chart: $Y = 54.906 + 2.2495*X + 5.946E\text{-}7*X^2$

FT: Flow Transducer
FC: Flow Controller
TWV: Three Way Valve
SP: Sampling Port
PG: Pressure Gauge
HFM: Hollow Fiber Module
VG: Vacuum Gauge
VP: Vacuum Pump
HC: Hydrocarbon Gas Cylinder
N_2: High Purity Nitrogen Gas Cylinder

Figure 15. Setup for Measurement of Hydrocarbon Permeance

CHAPTER 4

RESULTS AND DISCUSSION

4.1 Experimental Results

Experiments were primarily carried out in the tube-side feed mode. Since Celgard

membrane-based fibers (module #1) used for a majority of permeation studies carried out

for VOCs till now have yielded very good separation results (Cha, 1994; Malik, 1995),

it was decided to extend the use of these membranes for preliminary gasoline vapor

separation runs and compare the results with the performance of another membrane.

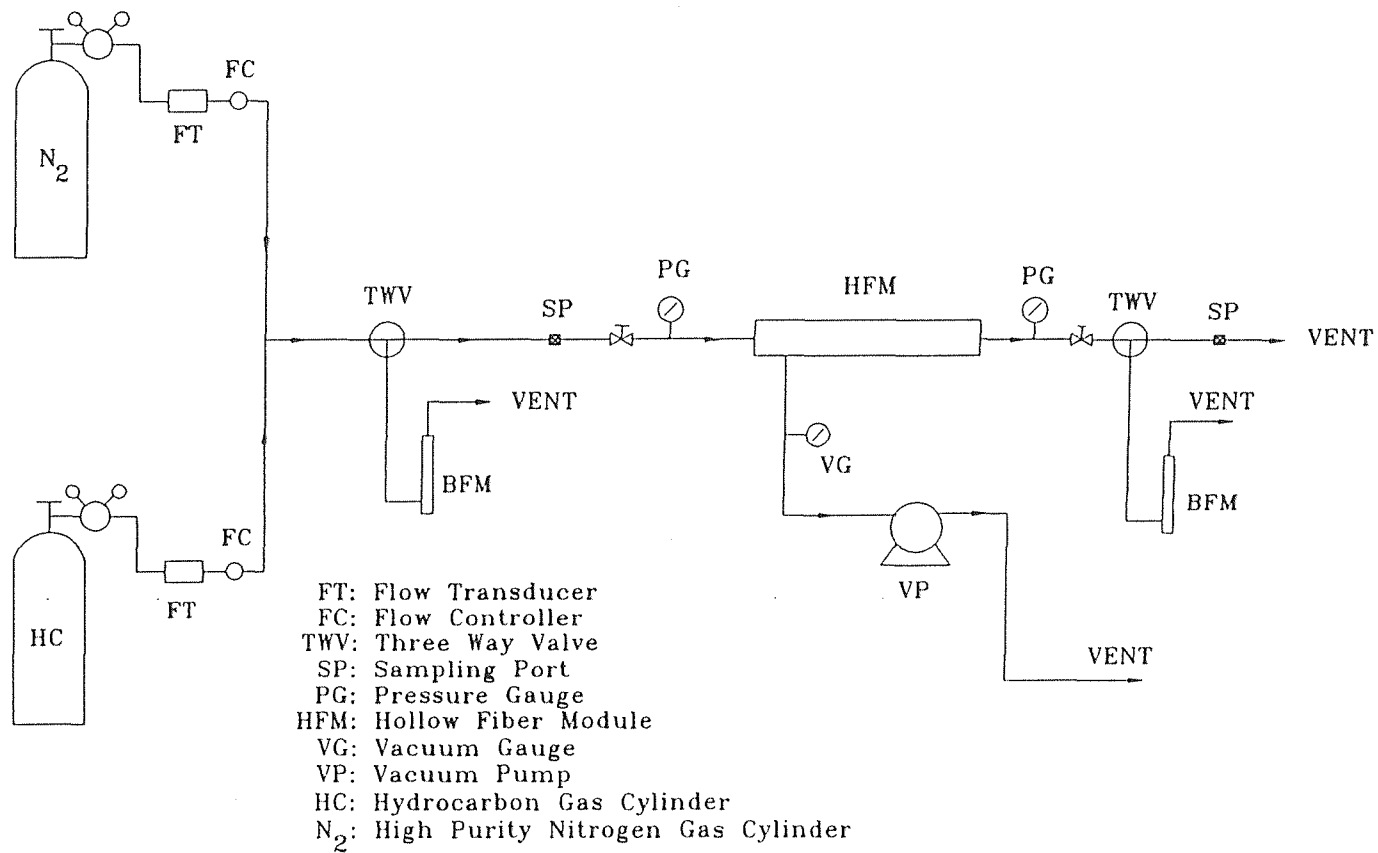Basic experimental parameters that were varied were feed flow rate, feed concentration,

permeate pressure and the type of membrane. Flow rates were varied from 5 cc/min to

100 cc/min using mass flow controllers. Desired concentrations could be achieved by

blending with nitrogen; the desired permeate pressure could be obtained by adjusting a

valve. The type of membrane was decided by the use of an appropriate module. Results

are summarized in Table 2 for membrane module #1.

Removal upto 99% could be achieved for all three hydrocarbons when the

operating flow rate was ~5 cc/min. Permeate fluxes decreased in the order of butane,

pentane and hexane (Figure 16), but still, were atleast, an order of magnitude lower than

nitrogen. At higher flow rates, percent removal decreased (Figure 17a) and as expected,

the selectivities increased (Figure 17b). Nitrogen flux was practically independent of flow

rate, but the hydrocarbon fluxes increased with flow rate, leading to higher selectivities.

Figures 17a and 18 also compare the extent of removal and treated gas concentrations

42

Table 2. Results of Gasoline Vapor Permeation (Module #1)

Feed Flow Rate (cc/min)	Retentate Gas Flow Rate (cc/min)	Feed Concentration (ppmv)			Retentate Concentration (ppmv)			Percent Removal		
		Butane	Pentane	Hexane	Butane	Pentane	Hexane	Butane	Pentane	Hexane
5.29	0.76	119300	40400	9980	5629	377	66	99.32	99.86	99.90
11.94	6.69	119300	40400	9980	38730	5729	350	81.81	92.05	98.04
16.24	10.63	119300	40400	9980	53146	9734	833	70.84	84.23	94.54
27.62	21.53	119300	40400	9980	79440	17518	2259	48.09	66.20	82.36
54.04	47.12	113000	39000	9950	86233	23454	3953	33.46	47.56	65.36
95.94	88.26	113000	39000	9950	97164	28875	5779	20.90	31.89	46.57

Permeate pressure = 1.0-1.5 cm Hg.
Tube-side feed mode.
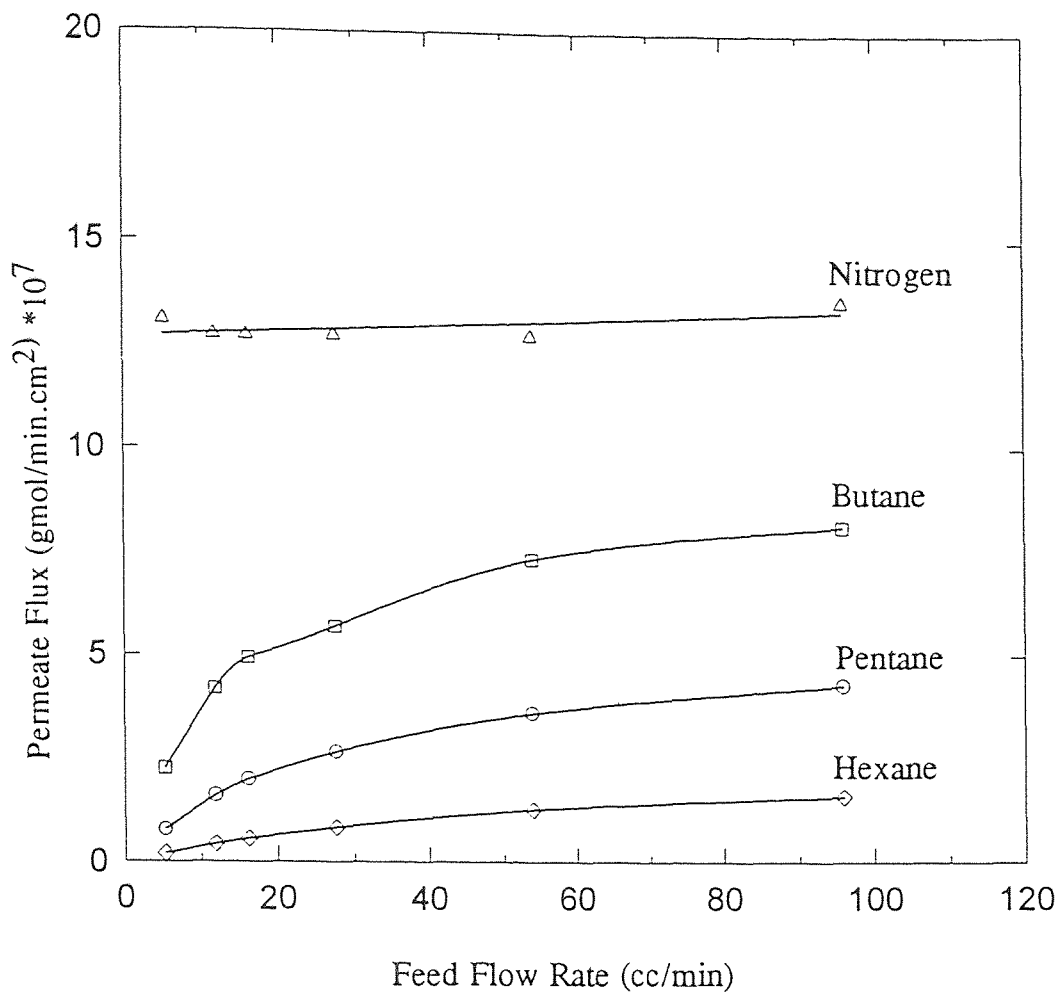
Feed Composition: ~ 12% Butane, 4% Pentane, 1% Hexane
balance Nitrogen
Module #1
Permeate pressure = 0.5-1.5 cm Hg

Figure 16. Variation of Flux with Flow Rate
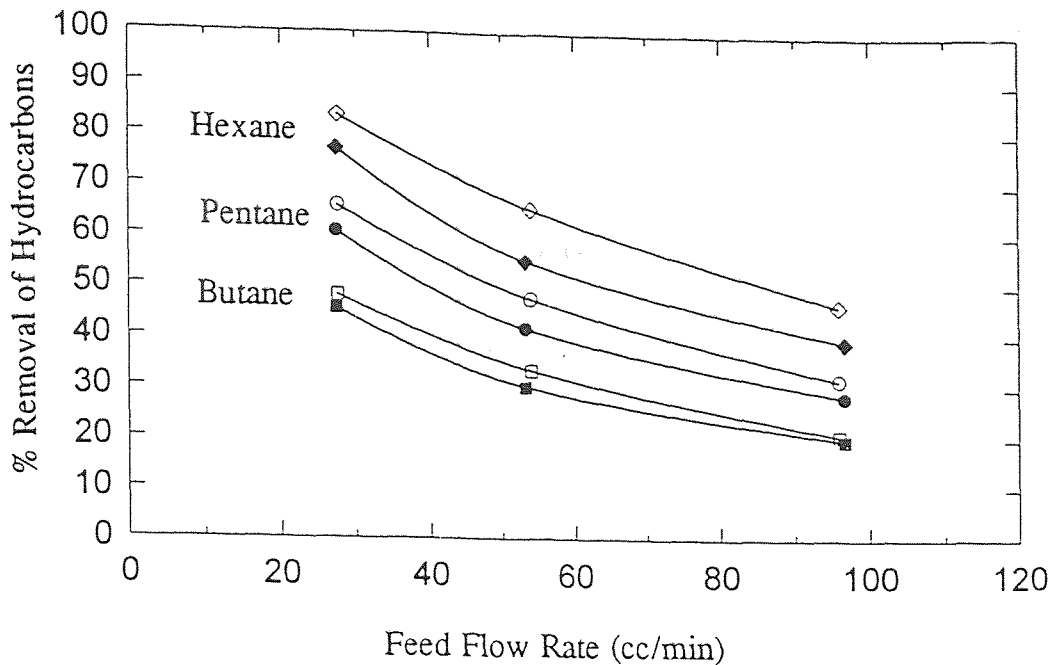
Figure 17a. Dependence of Removal of Hydrocarbons on Flow Rate
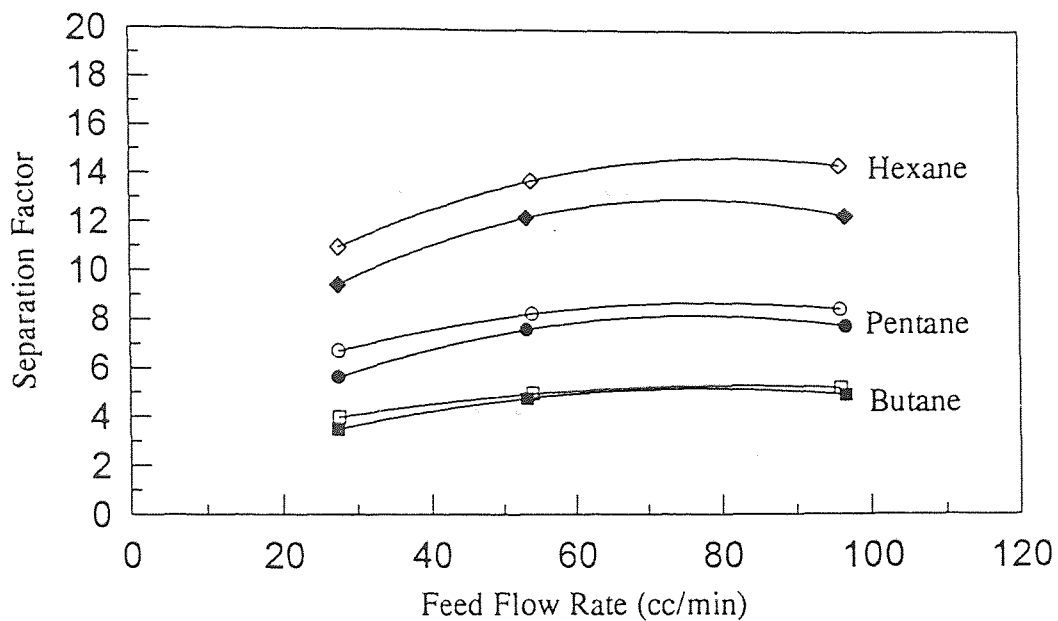
Figure 17b. Influence of Flow Rate and Permeate Pressure on Selectivity

Feed Composition: ~12% Butane, 4% Pentane, 1% Hexane
balance Nitrogen
Module #1

o   : Permeate Pressure = ~2.0 cm Hg
●   : Permeate Pressure = ~5.5 cm Hg
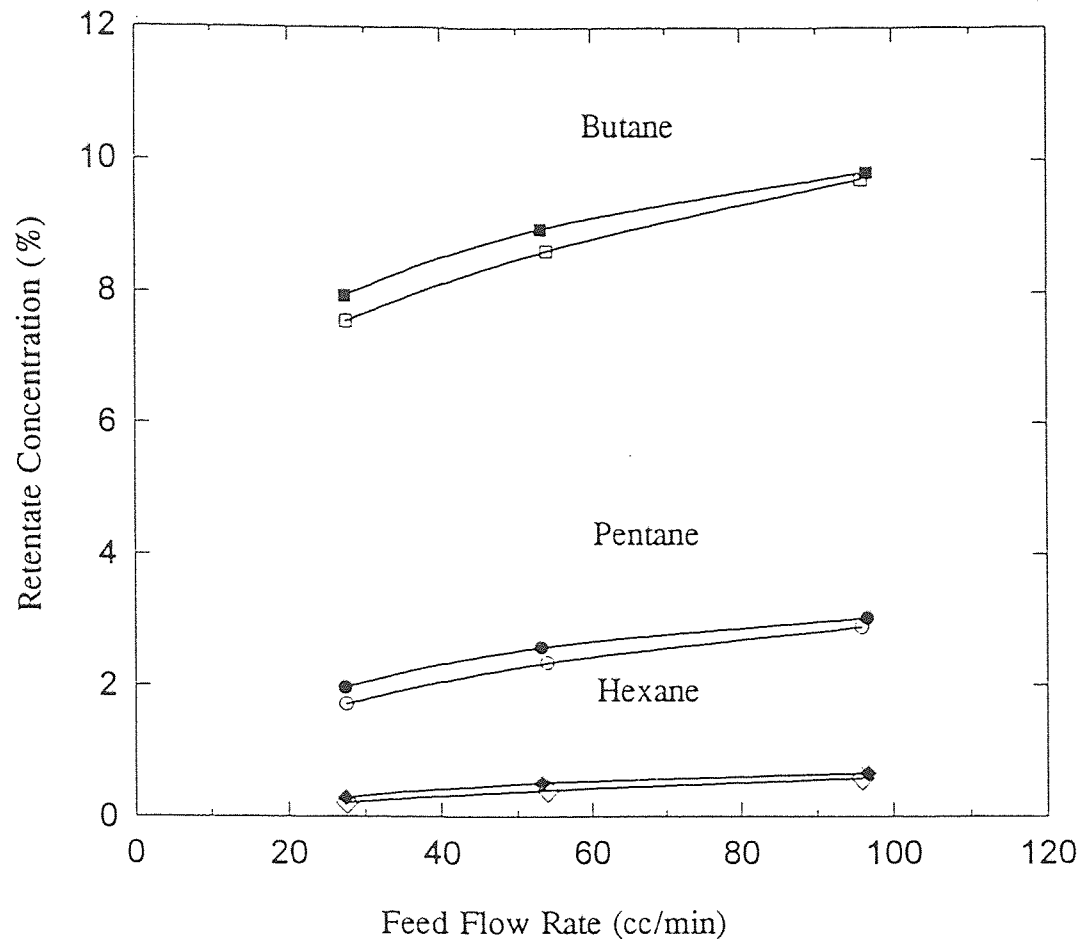
Feed Composition: ~12% Butane, 4% Pentane, 1% Hexane
balance Nitrogen

Module #1

○   : Permeate Pressure = ~2.0 cm Hg
●   : Permeate Pressure = ~5.5 cm Hg

Figure 18. Outlet Concentration Vs. Feed Flow Rate

as a function of the permeate pressure. The performance of the module was marginally better in the case of lower permeate pressure (higher level of vacuum) since the driving force (partial pressure difference) was higher. To obtain lower concentrations at the outlet, the feed gas (~ 12% butane, ~ 4% pentane, ~ 1% hexane, ~ 83% nitrogen) was also blended with pure nitrogen in the ratio 1:1. For the same molar flow rate of hydrocarbons, lower retentate concentrations could be obtained for feed blended with nitrogen (refer to Table 3).

Better separation was obtained when the feed was introduced from the tube side with vacuum on the shell side instead of the shell side feed mode. This could be because of higher permeate pressure drop when vaccum is being maintained on the tube side, while there is no significant pressure drop on the feed side in either mode. Results for the shell-side feed are shown in Table 4.

To study the effect of immobilizing a suitable liquid in the pore, experiments were performed with the Hamilton Standard module (module #5). Two base-line data points were obtained without immobilizing any liquid and two other data points after immobilizing (Table 5) PEG and PEGDE (a derivative of PEG) in the pores, separately. Nitrogen flux was drastically cut down from ~ 35 cc/min to ~ 0.07 cc/min while the hydrocarbon fluxes were reduced by only two orders of magnitude, resulting in higher selectivities. Feed flow rates were as low as 5 cc/min, but hydrocarbon removal higher than 20% could not be achieved. A comparison of the module performance with the derivative (PEGDE) immobilized in the pores, showed that PEG results in a better immobilized liquid membrane than PEGDE. The drastic change in the performance of the module after liquid immobilization is evident from Figures 19 and 20.

Table 3. Results of Gasoline Vapor Permeation with Higher Permeate Pressure and Blending (Module #1)

Feed Flow Rate (cc/min)	Retentate Gas Flow Rate (cc/min)	Feed Concentration (ppmv)			Retentate Concentration (ppmv)			Percent Removal		
		Butane	Pentane	Hexane	Butane	Pentane	Hexane	Butane	Pentane	Hexane
27.38*	21.25	113000	39000	9950	79417	19734	2941	45.45	60.73	77.06
53.25*	46.89	113000	39000	9950	89579	25824	5071	30.20	41.69	55.12
96.64*	89.02	113000	39000	9950	98190	30256	6554	19.96	28.54	39.32
26.71+	20.29	55562	19177	4892	41032	10047	1402	43.90	60.20	78.24
54.85+	49.50	55325	19095	4872	47224	13551	2533	22.97	35.96	53.08

* Experiments with higher permeate pressure (~5.5 cm Hg).
+ Experiments with gasoline diluted with nitrogen.
Tube-side feed mode.

Table 4. Results of Gasoline Vapor Permeation with Feed Introduced from the Shell-side (Module #1)

Feed Flow Rate (cc/min)	Retentate Gas Flow Rate (cc/min)	Feed Concentration (ppmv)			Retentate Concentration (ppmv)			Percent Removal		
		Butane	Pentane	Hexane	Butane	Pentane	Hexane	Butane	Pentane	Hexane
15.75	11.08	119000	39300	10000	67986	14984	1845	59.81	73.18	87.02
27.31	21.67	119000	39300	10000	83030	21828	3623	44.63	55.92	71.25
27.28*	22.48	119000	39300	10000	82808	21781	3678	42.67	54.34	69.70
53.22	47.54	119000	39300	10000	97367	29034	5937	26.91	34.01	46.96
56.17*	50.13	119000	39300	10000	94872	28294	5763	28.85	35.75	48.57
97.88	91.79	119000	39300	10000	102533	31952	7073	19.20	23.76	33.67

* Experiments done in countercurrent mode of operation.
Permeate pressure = 0.3-1.4 cm Hg.

Table 5. Results of Gasoline Vapor Permeation With and Without Immobilization (Module #5)

Feed Flow Rate (cc/min)	Retentate Gas Flow Rate (cc/min)	Feed Concentration (ppmv)			Retentate Concentration (ppmv)			Selectivity w.r.t N_2		
		Butane	Pentane	Hexane	Butane	Pentane	Hexane	Butane	Pentane	Hexane
61.15	18.29	119700	39300	10000	119515	37538	8727	1.01	1.05	1.13
97.40	56.29	119700	39300	10000	118918	36734	8281	1.02	1.14	1.37
5.02*	4.83	119700	39300	10000	108539	33558	8241	8.39	12.35	14.78
9.58*	9.31	119700	39300	10000	110672	34484	8623	10.74	16.36	18.29
6.40+	5.92	119700	39300	10000	106598	32090	7478	3.88	5.70	7.60
9.48+	8.93	119700	39300	10000	108686	33352	8113	4.27	6.19	7.49

* Celgard membrane immobilized with polyethylene glycol.
+ Celgard membrane immobilized with polyethylene glycol dimethyl ether.
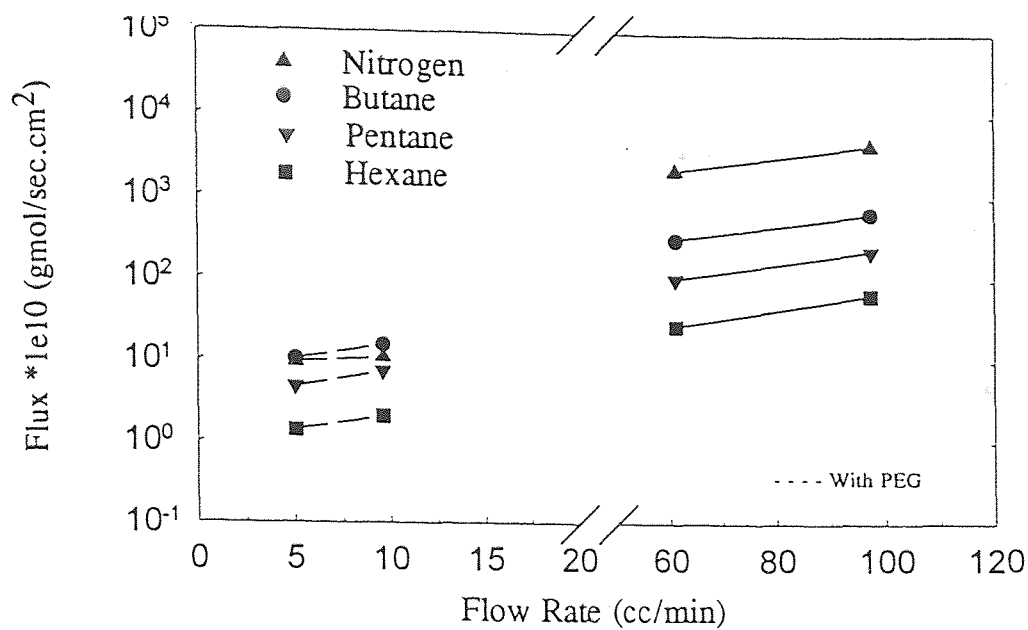Tube-side feed mode. Permeate pressure = 1.0-2.0 cm Hg.

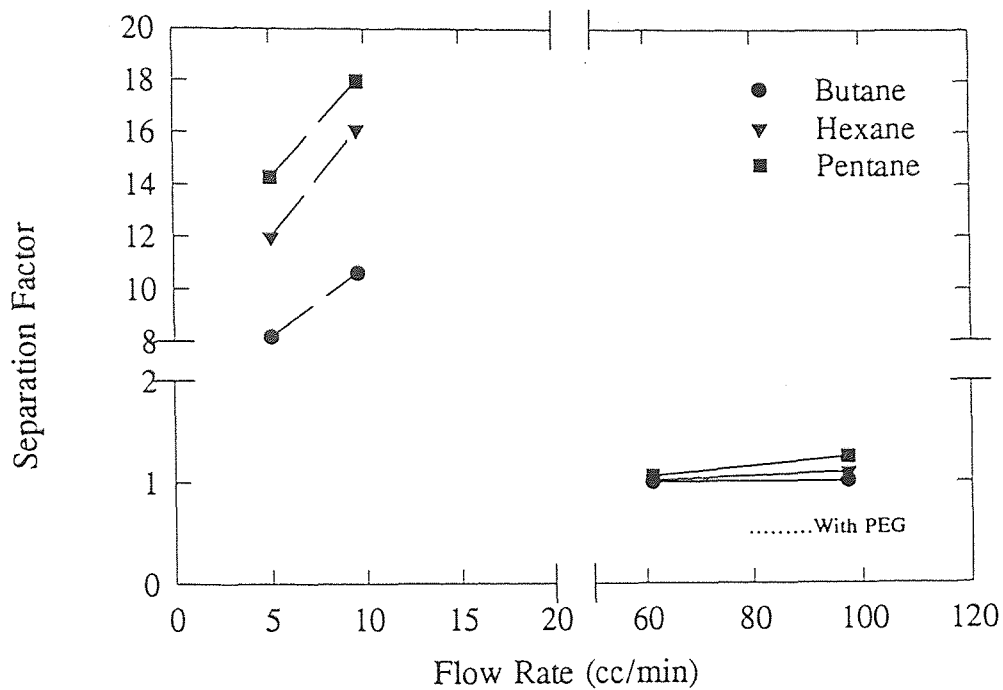**Figure 19.** Effect of Immobilization on Variation of Flux (Module #5)

Figure 20. Effect of Immobilization on Separation Factor (Module #5)

With the Mitsubishi support-based coated membrane (module #3), ~95% of the hydrocarbons could be removed at a flow rate of 30 cc/min (selectivities varied from 3 to 8), but unlike the Celgard-based membrane, nitrogen permeation was high. Upon liquid immobilization in the Mitsubishi membrane (module #3), feed flow rates had to be decreased because of low nitrogen permeation rates (~0.7 cc/min). Influence of using an immobilized liquid membrane, instead of just the composite membrane, on species flux and respective separation factors is shown in Figures 21 and 22. Nitrogen, as well as hydrocarbon fluxes, were reduced by the same order of magnitude, resulting in similar separation factors as before immobilization. When the experiments were repeated with the same module (module #3) after washing off PEG from the pores, the separation behavior was different. 92-93% of the hydrocarbons could be removed at flow rates of 30 cc/min, but the separation factors were higher (6-16) than in the previous case. This could be due to the presence of a thin film of the immobilized liquid in the polypropylene substrate, even after repeated attempts to wash off PEG from the pores. With module #2 (silicone fluoropolymer coating), ~95% of hydrocarbons could be removed at a flow rate of 55 cc/min with separation factors ranging from 3 to 8. These results are summarized in Table 6 and illustrated in Figures 23 and 24.

A comparison of this work with similar work done at GKSS with more expensive flat membranes (Ohlrogge et al., 1995) is shown in Figures 25 and 26. Unlike this work, the effect of stage cut has not been studied in their work. Performance similar to GKSS modules could be achieved at the same operating stage cut.

Permeances of individual components were also obtained through a separate set of experiments with binary mixtures (hydrocarbon and nitrogen) using module #6. From

Table 6. Results of Gasoline Vapor Permeation With and Without Immobilization (Module #3 & #4)

Feed Flow Rate (cc/min)	Retentate Gas Flow Rate (cc/min)	Feed Concentration (ppmv)			Retentate Concentration (ppmv)			Percent Removal		
		Butane	Pentane	Hexane	Butane	Pentane	Hexane	Butane	Pentane	Hexane
29.87	10.80	117000	40000	10000	31260	3462	126	90.34	96.87	99.54
55.15	34.78	117000	40000	10000	64868	13021	1254	65.03	79.47	92.09
5.22*	4.23	117000	40000	10000	101858	30750	6275	29.41	37.67	49.12
55.98*	55.16	117000	40000	10000	116104	39072	9486	2.22	3.75	6.53
11.89+	2.84	117000	40000	10000	3291	99	5	99.33	99.94	99.98
20.37+	11.78	117000	40000	10000	19572	1583	50	90.32	97.71	99.71
28.50+	17.99	117000	40000	10000	34619	4346	198	81.31	93.14	98.74
55.66#	15.15	119700	39900	10000	29498	2933	86	93.29	97.99	99.77
72.73#	33.21	119700	39900	10000	48017	6651	326	81.68	92.39	98.51

* Mitsubishi membrane (silicone-hydrocarbon coating) immobilized with polyethylene glycol.
+ Mitsubishi membrane (silicone-hydrocarbon coating) after washing off immobilized polyethylene glycol.
# Mitsubishi membrane (silicone-fluoropolymer coating).
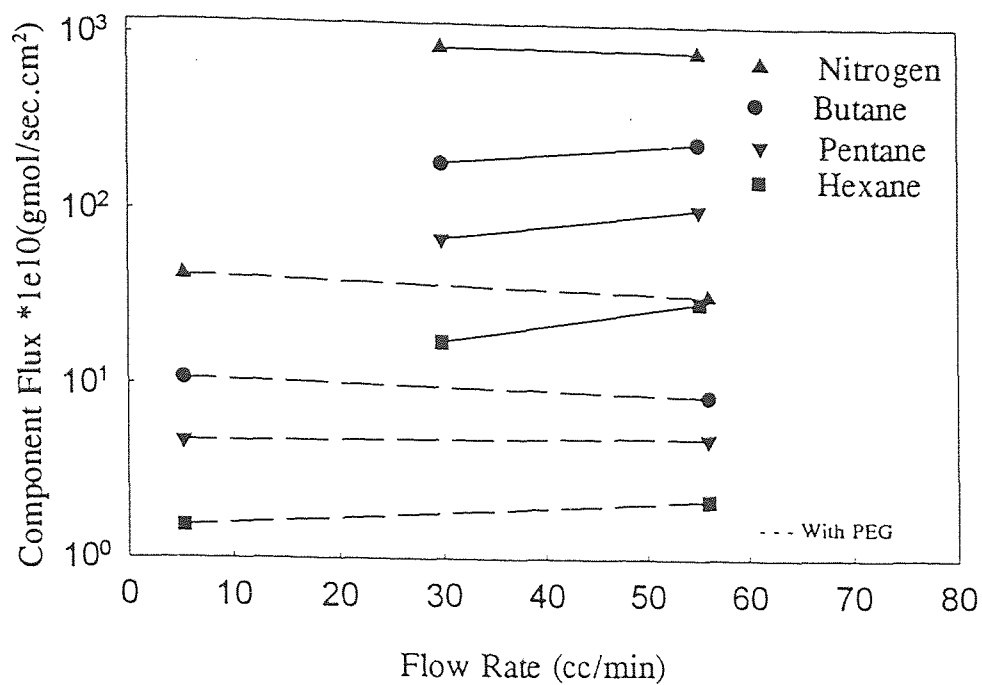Tube-side feed mode.
Permeate pressure = 0.3-2.8 cm Hg.

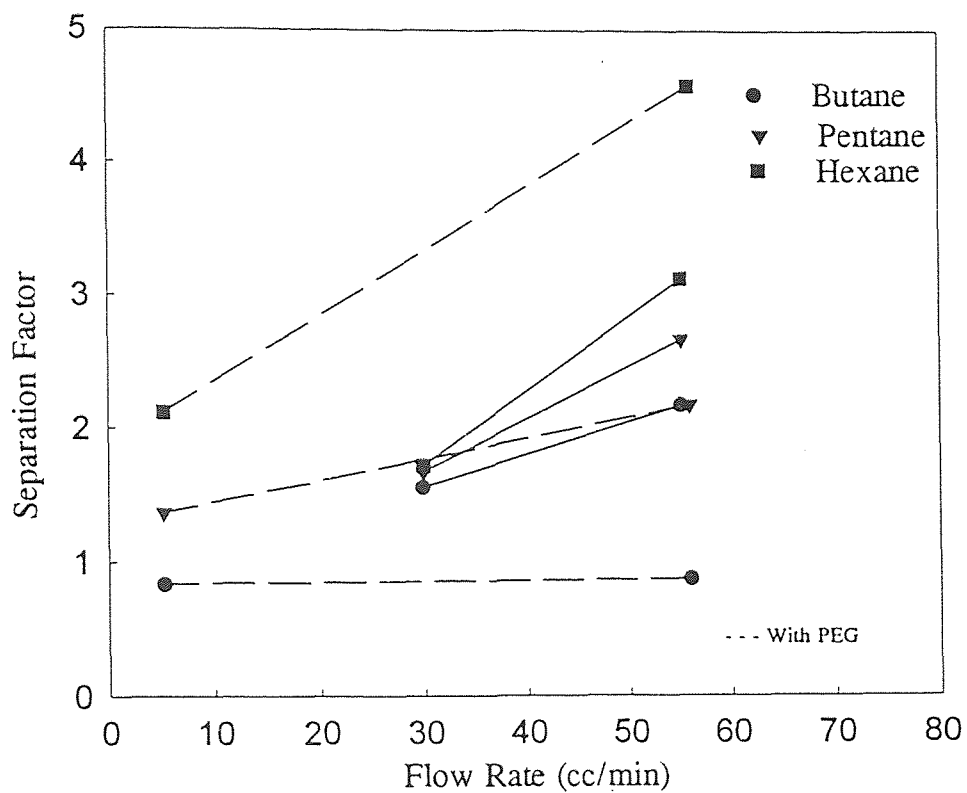**Figure 21.** Effect of Immobilization on Variation of Flux (Module #3)

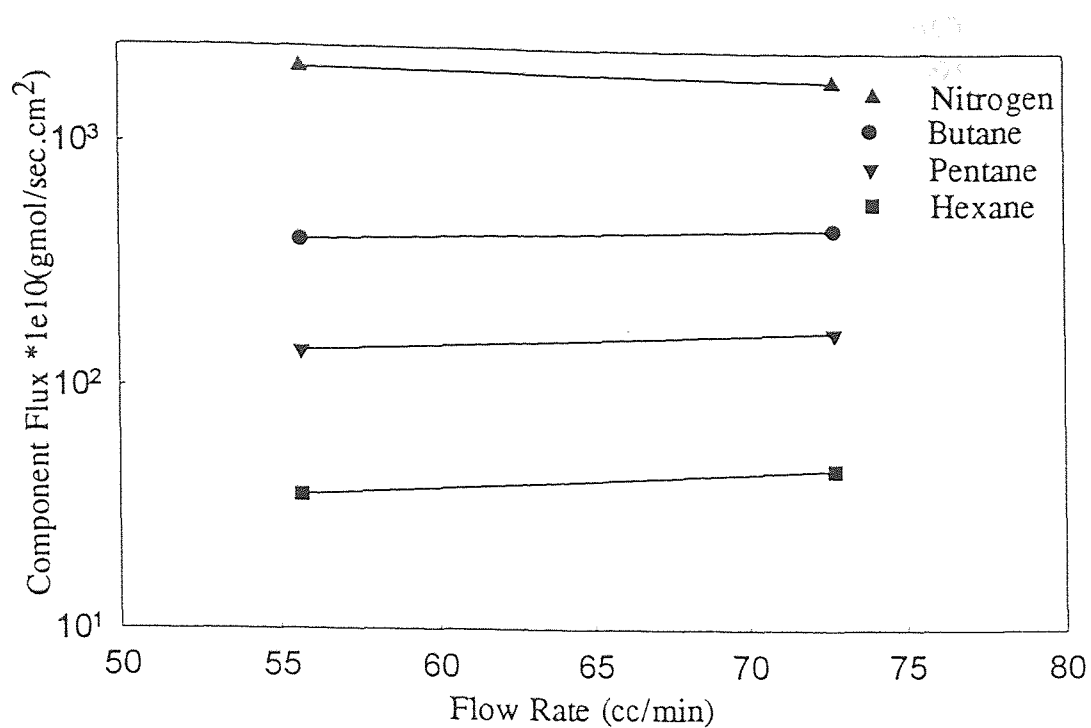**Figure 22.** Effect of Immobilization on Separation Factor (Module #3)

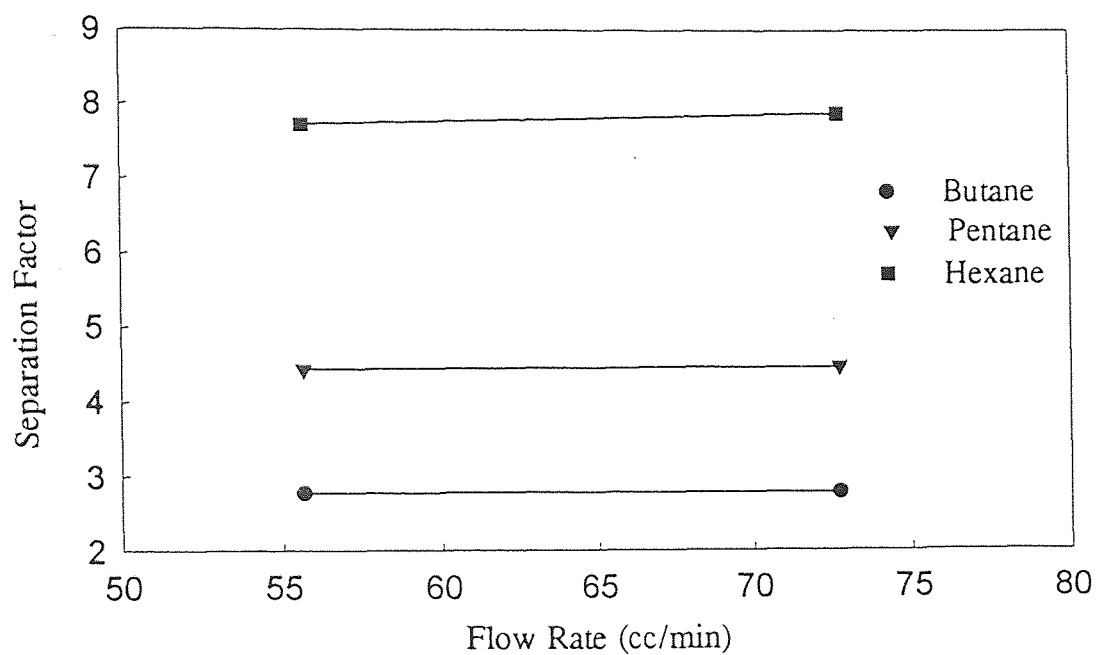**Figure 23.** Variation of Flux with Flow Rate (Module #2)

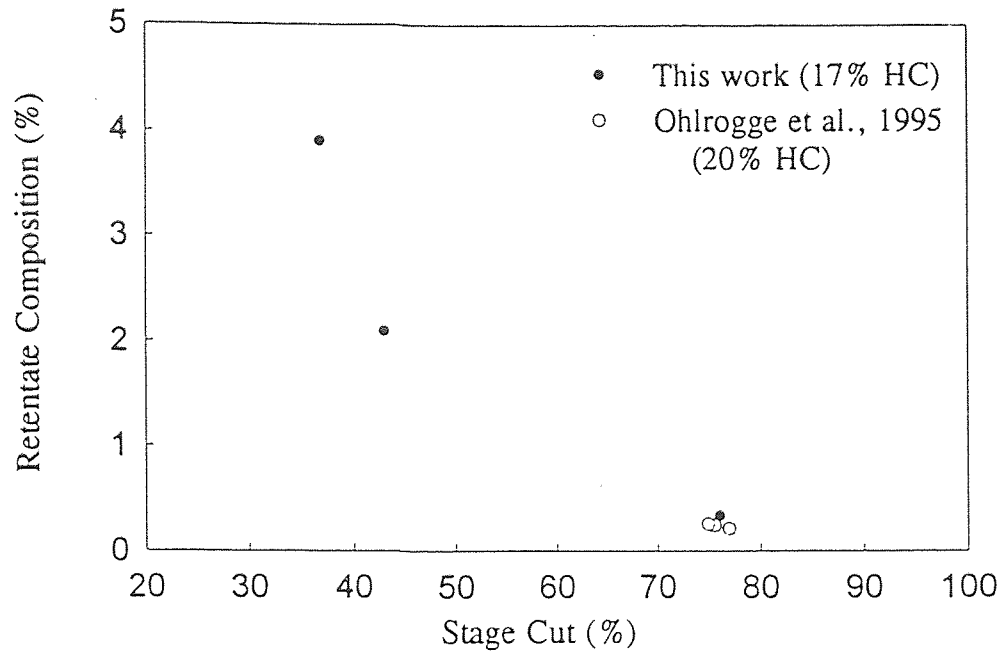**Figure 24.** Variation of Separation Factor with Flow Rate (Module #2)

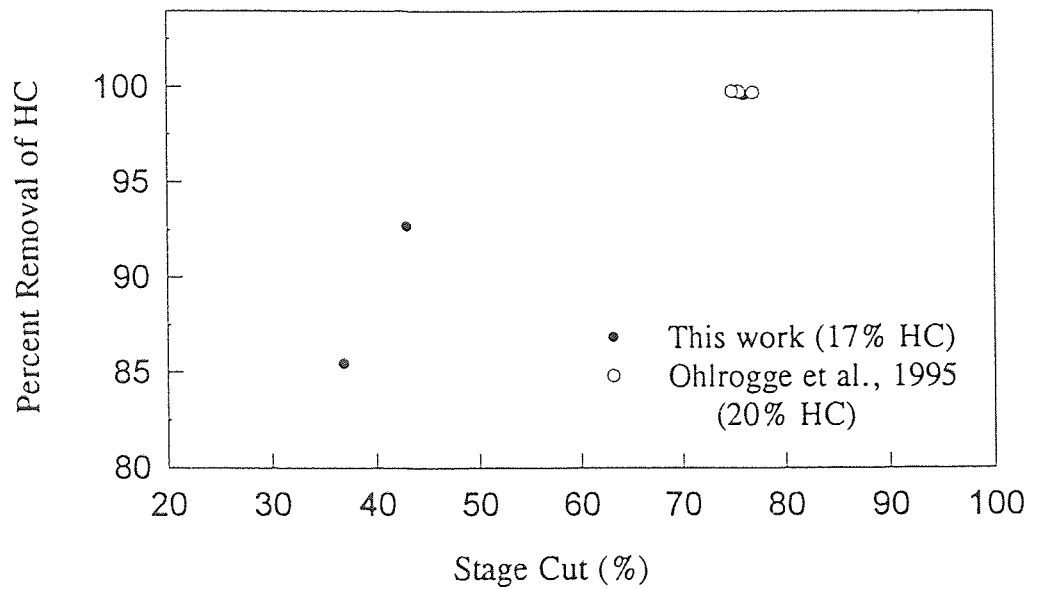**Figure 25.** Comparison of Variation in Retentate Concentration

Figure 26. Comparison of Variation in Removal of Hydrocarbons

Module #1
Permeate pressure = 1-2 cm Hg

Figures 27, 28 and 29, it could be seen that the presence of other hydrocarbons marginally increases the permeance of each species, as opposed to the permeance measured in the presence of only an inert permeating species (like nitrogen). It could be concluded that the presence of other organics creates an environment which favors permeation of these hydrocarbons in the pores of the composite membrane, by decreasing the resistance to mass transfer, whereas the permeance of nitrogen is practically independent of such an effect. It should be remembered that, in each case, the total organic solvent level was higher when other organics were present.

Binary mixtures of nitrogen and individual hydrocarbons were also used as feed for separation studies (see Tables 7, 8 and 9) and to generate experimental data for simulation. Figures 30, 31 and 32 illustrate the influence of presence of permeating organics on species removal. The trend, as expected, is similar to that observed for permeance variation. It has also been observed that the percent removal of organics is, in general, independent of concentration and depends only on the flow rate.

4.2 Modeling Results

The mathematical model described in Chapter 2.2 was applied to the case of binary mixture permeation. A FORTRAN code was written to execute the iterations. The code involved calling an IMSL (International Mathematical and Statistical Library) subroutine called NEQNF. This subroutine solves a fixed number of algebraic equations for the same number of unknown variables by a finite difference method. A typical sample of the program executed is provided in Apppendix B. The same program has been used to simulate data in both operational modes (shell-side feed and tube-side feed).
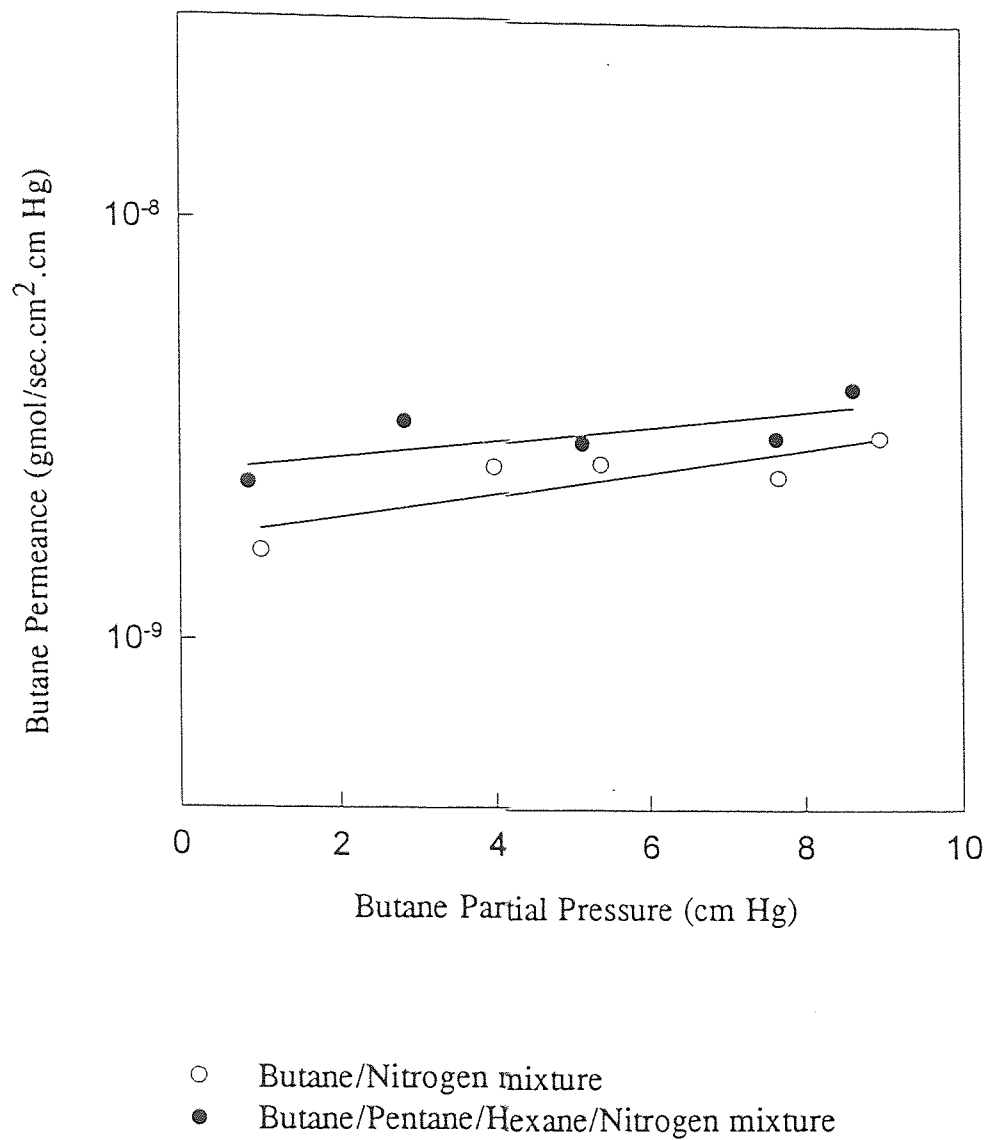
○   Butane/Nitrogen mixture
●   Butane/Pentane/Hexane/Nitrogen mixture

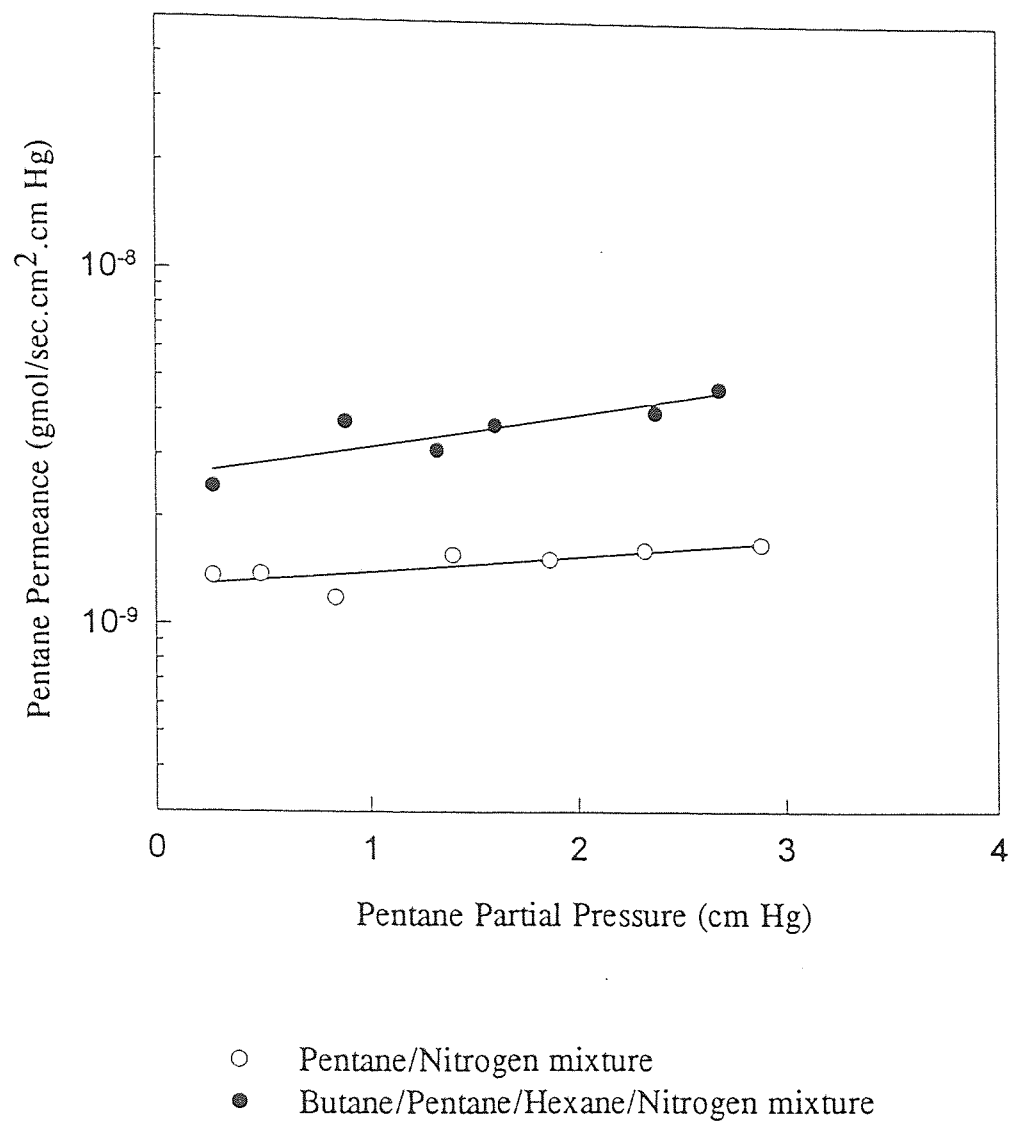**Figure 27.** Dependence of Butane Permeance on Feed Partial Pressure

Figure 28. Variation of Pentane Permeance with Feed Partial Pressure
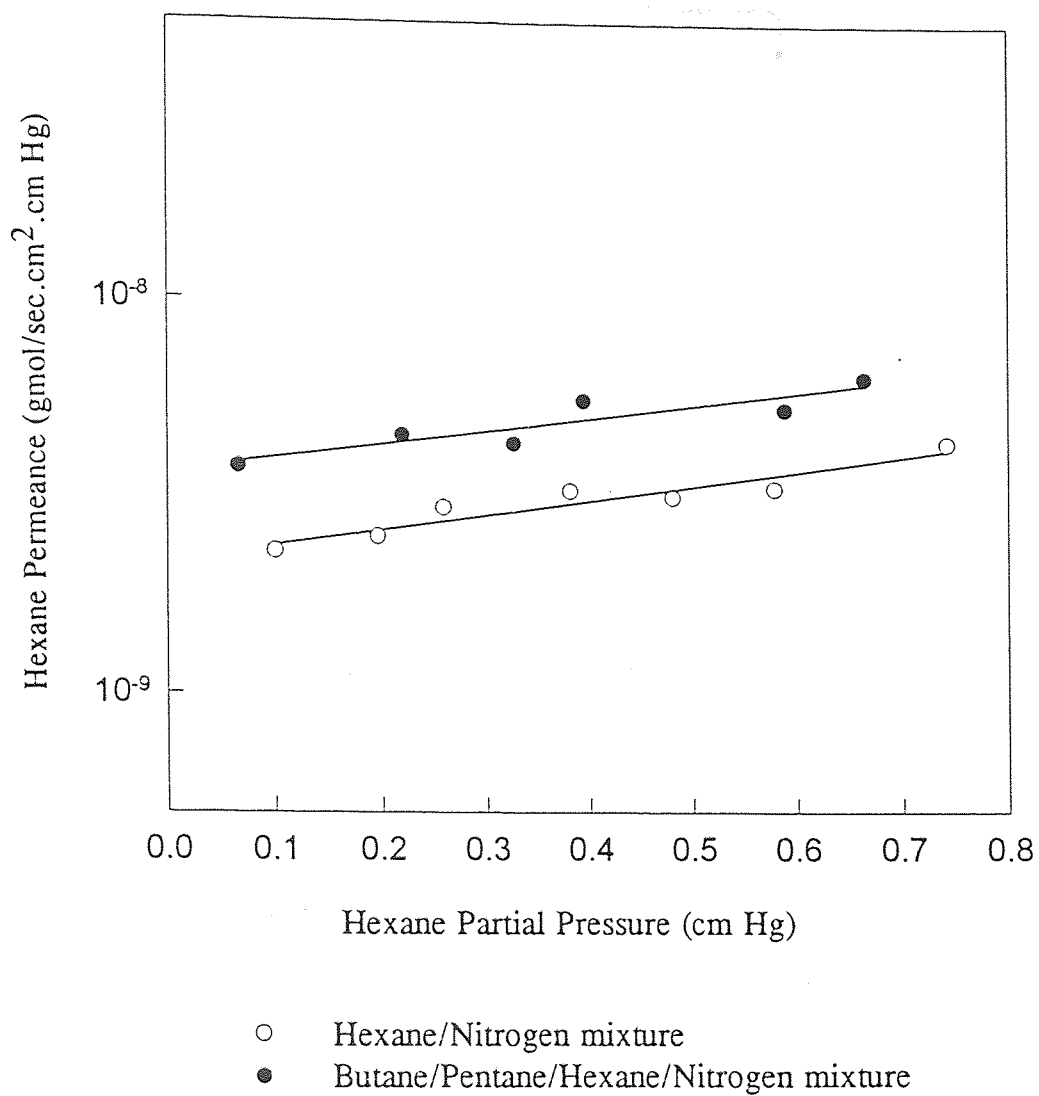
Figure 29. Dependence of Hexane Permeance on Partial Pressure

Table 7. Results of Butane/ Nitrogen Vapor Separation (Module #4)

Feed Flow Rate (cc/min)	Treated Gas Flow Rate (cc/min)	Butane Inlet Concentration (ppmv)	Butane Outlet Concentration (ppmv)	Percent Removal
38.12	32.91	120000	86499	37.78
63.47	58.19	120000	99467	24.00
96.93	91.58	120000	108264	14.76
61.73*	56.67	37276	31594	22.19
63.58*	58.40	57376	49236	21.18
61.57*	56.39	59627	50094	23.05
60.40*	55.07	91408	77384	22.81

* Feed blended with nitrogen.
Tube-side feed mode.
Permeate pressure = 0.7-1.3 cm Hg.

Table 8. Results of Pentane/Nitrogen Vapor Separation (Module #4)

Feed Flow Rate (cc/min)	Treated Gas Flow Rate (cc/min)	Pentane Inlet Concentration (ppmv)	Pentane Outlet Concentration (ppmv)	Percent Removal
29.43	24.88	38000	20129	55.22
61.54	56.81	38000	27812	32.44
99.42	95.04	38000	31049	21.89
64.74*	59.67	28384	20898	32.15
61.38*	56.65	24669	18096	32.29
62.83*	57.79	20404	14888	32.89
60.02*	55.65	9675	7316	29.88

* Feed blended with nitrogen.
Tube-side feed mode.
Permeate pressure = 0.8-1.7 cm Hg

Table 9. Results of Hexane/Nitrogen Vapor Separation (Module #4)

Feed Flow Rate (cc/min)	Treated Gas Flow Rate (cc/min)	Hexane Inlet Concentration (ppmv)	Hexane Outlet Concentration (ppmv)	Percent Removal
34.63	29.53	9770	3481	69.61
61.36	56.60	9770	5631	46.83
98.68	93.93	9770	6935	32.43
62.73*	57.93	6004	3586	44.85
61.55*	56.78	4679	2763	45.53
64.17*	59.48	3357	2033	43.86

* Feed blended with nitrogen.
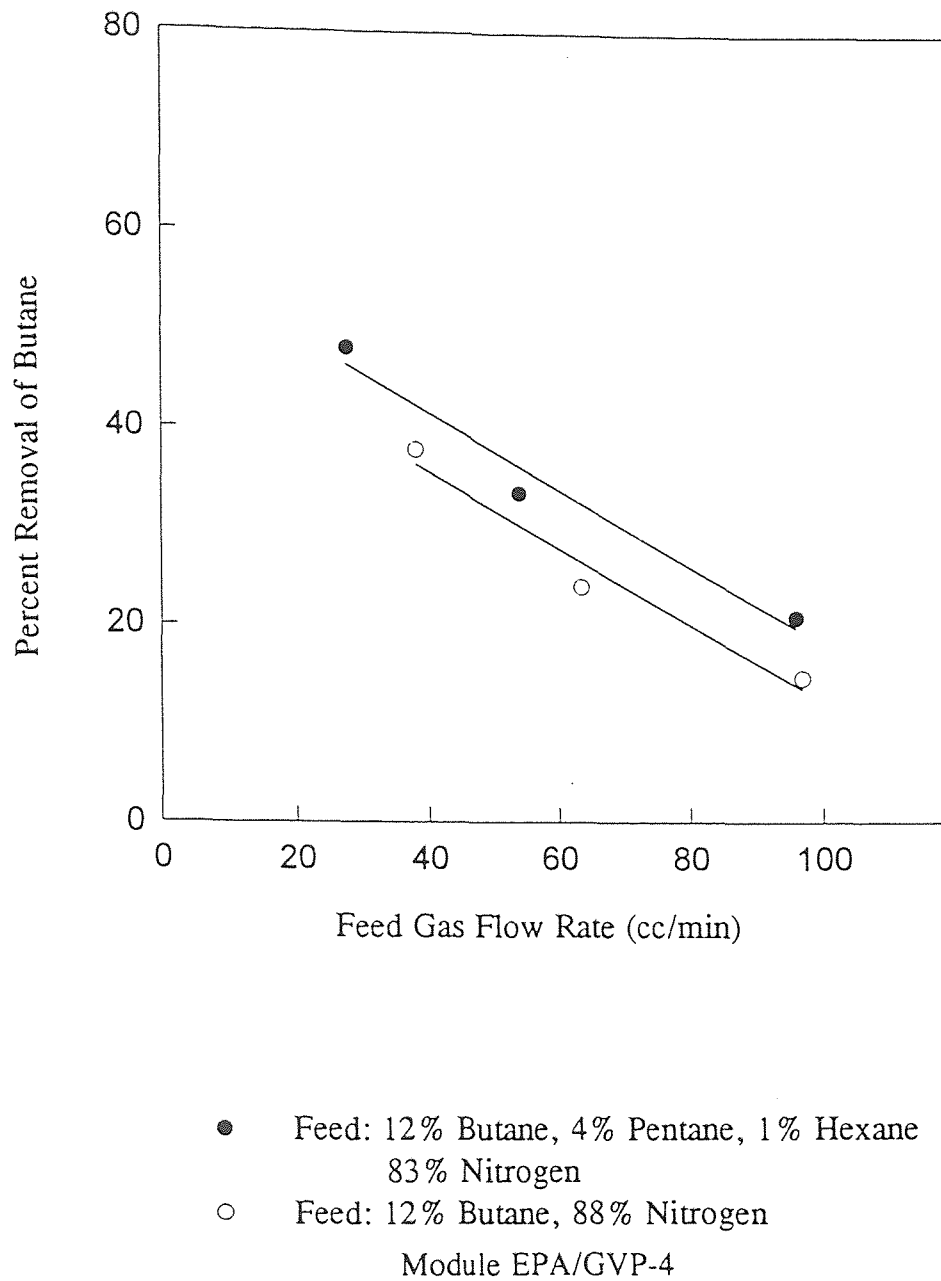Tube-side feed mode.
Permeate pressure = 1.0-1.8 cm Hg.

Figure 30. Influence of Other Hydrocarbons on Removal of Butane

Feed: 12% Butane, 4% Pentane, 1% Hexane
83% Nitrogen
Feed: 4% Pentane, 96% Nitrogen
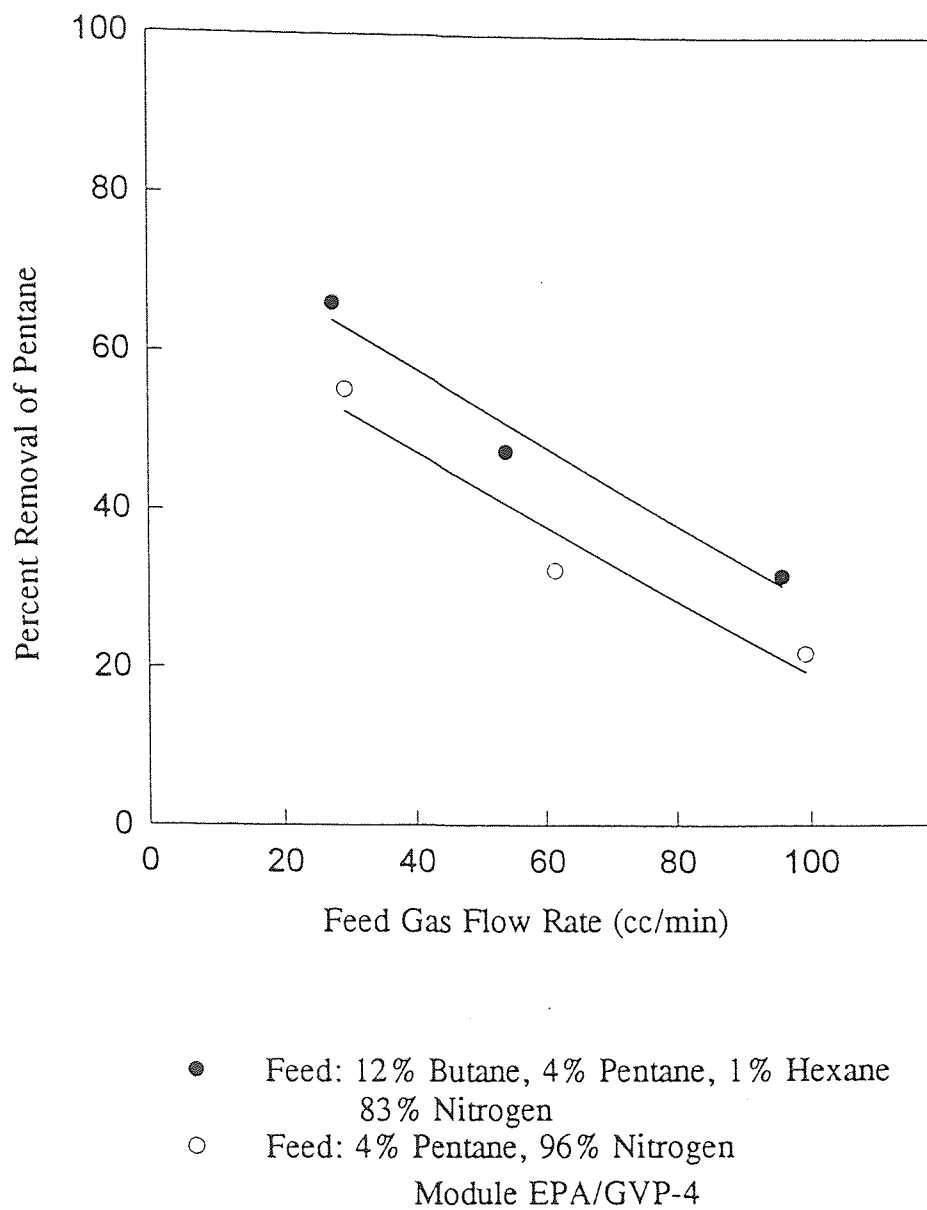Module EPA/GVP-4

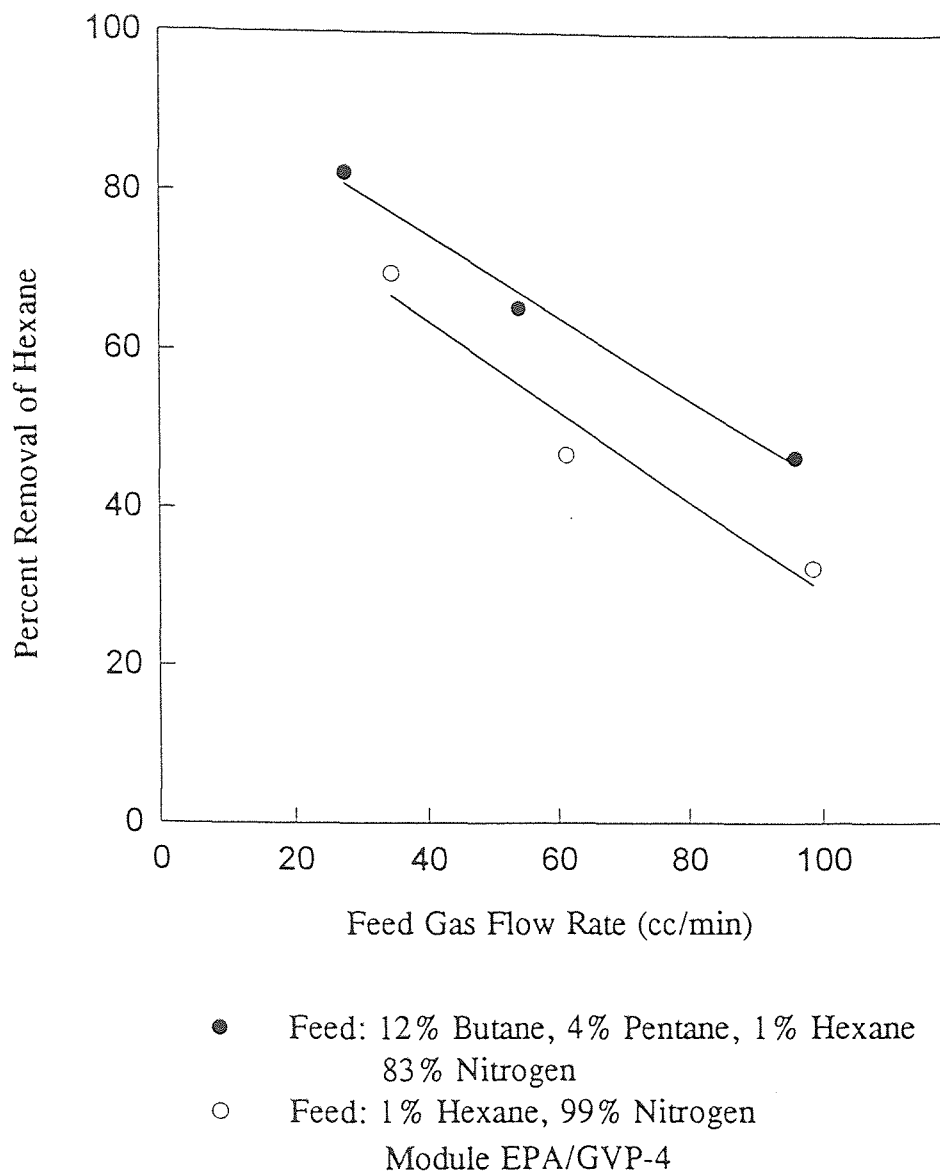Figure 31. Influence of Other Components on Removal of Pentane

Figure 32. Influence of Other Hydrocarbons on Removal of Hexane

The functional dependence of the permeance of an organic species on its concentration has been incorporated in solving the permeation equations. Permeation-separation data generated for toluene and methanol by Cha (1994) and Malik (1995) for both, shell-side and tube-side feed, were used to establish the validity of the model. To account for the pressure drop in the substrate, it has been assumed somewhat arbitrarily, that the substrate consists of pores with a radius of 2.5 °A and a length of 2.5 μm. This structure of the substrate is based on the fact that during the plasma polymerization process, the depostion also penetrates into the pore and forms a uniform coating on the inner walls. In analogy, work done by Xomeritakis and Lin (1994) on modified counterdiffusion chemical vapor deposition (MCVD) has proved that the deposition diffuses into the membrane pores and plugs the pores. Pressure drop in other sections of the substrate with larger radii (100-300 °A) is inversely proportional to the radius of the pore and is negligible compared to the pressure drop in the semi-plugged section.

$$\Delta P \; \alpha \; \frac{1}{r_p}$$

Figures 33 and 34 compare the results of the program with experimental results for toluene. There is considerable difference in the treated gas composition in the two modes. This could be due to two reasons.

a. Comparing the two modes of operation, feed side pressure drop is negligible, but the permeate pressure drop is higher in the case of vaccum on the tube side (i.e shell-side feed).
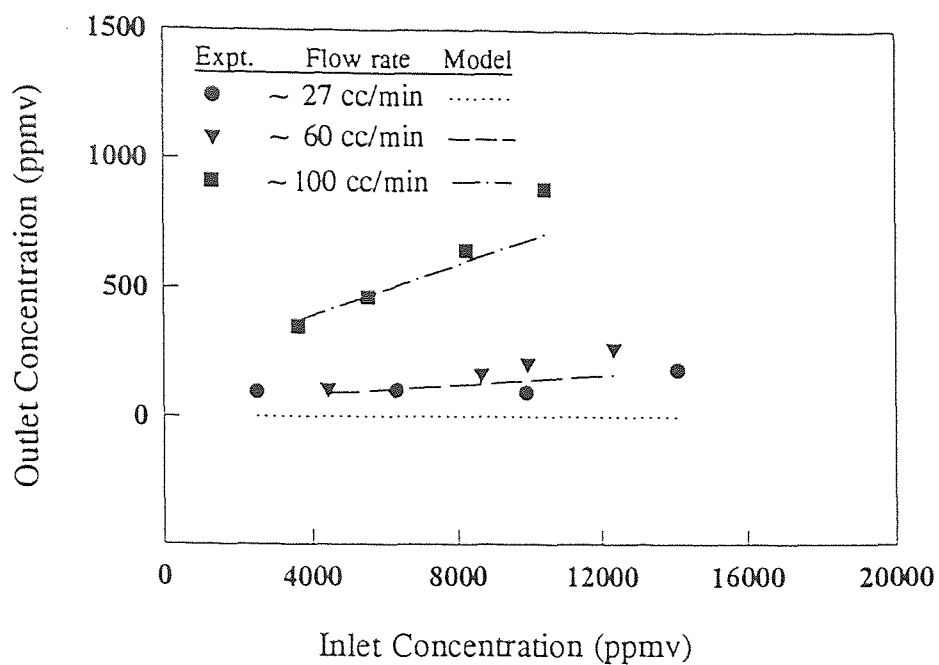
Figure 33. Comparison of Experimental and Modeling Results
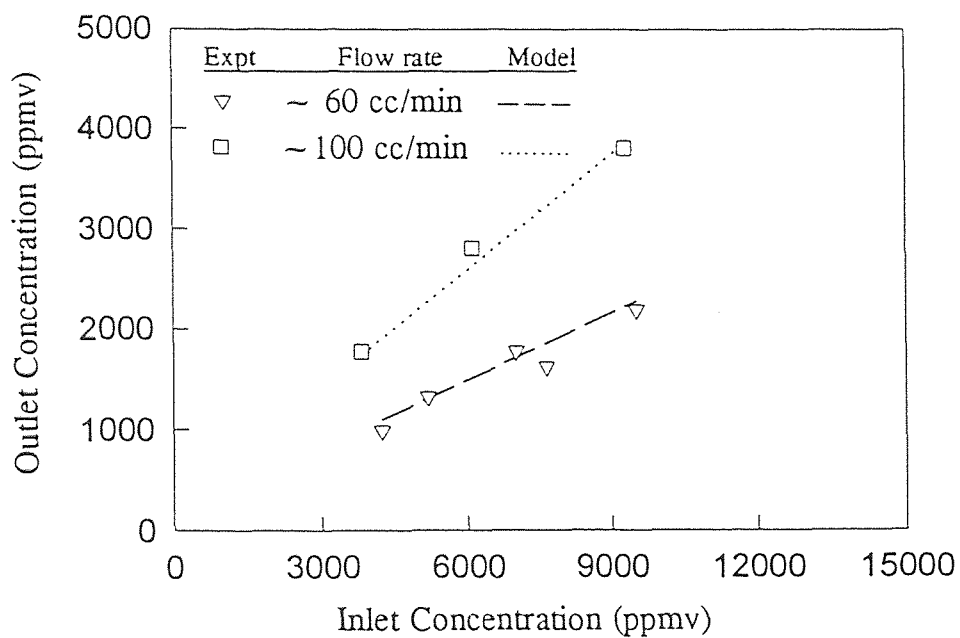for Toluene for Tube-side Feed

Figure 34. Comparison of Experimental and Modeling Results
for Toluene for Shell-side Feed

b. Coupled to this effect is the pressure drop in the substrate, in the shell side feed mode.

Figure 35, an illustration of the results for methanol, also shows that the difference in the two modes increases more at higher concentrations. It should be noted that methanol permeance data were not available beyond 50,000 ppmv. Figures 36-41 show the results for butane, pentane and hexane in the tube side feed mode. Appendix C provides the individual permeance data used in modeling for each species. For all these simulation results, the outlet gas flow rate varied within 1% of the experimental data.
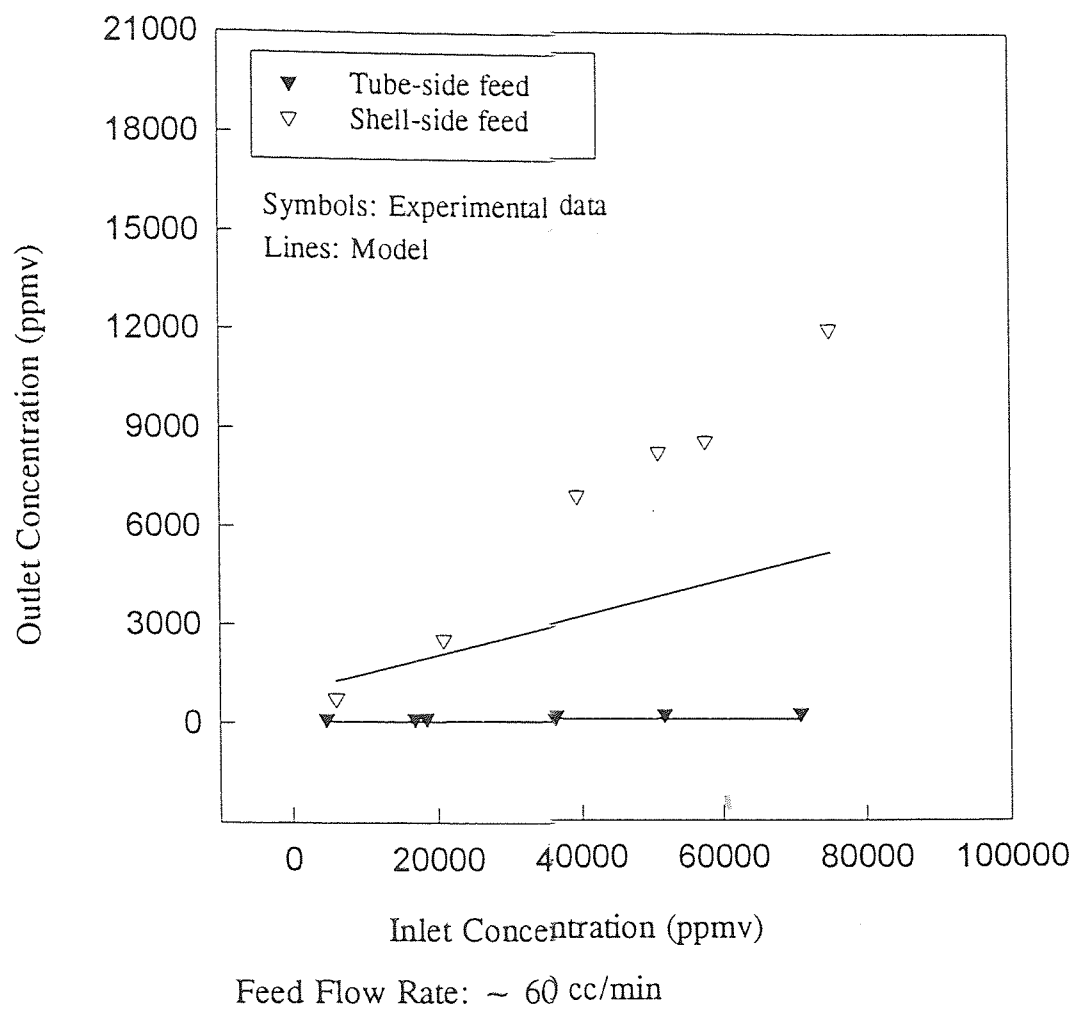
Figure 35. Experimental and Modeling Results for Methanol
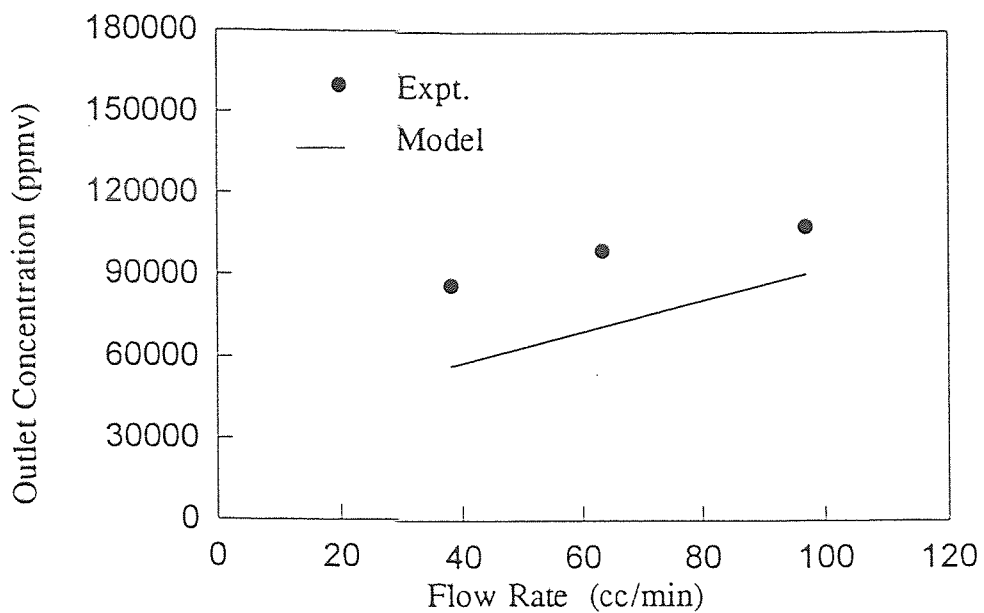
Feed Concentration: 12% Butane
88% Nitrogen

Figure 36. Variation of Butane Concentration with Flow Rate
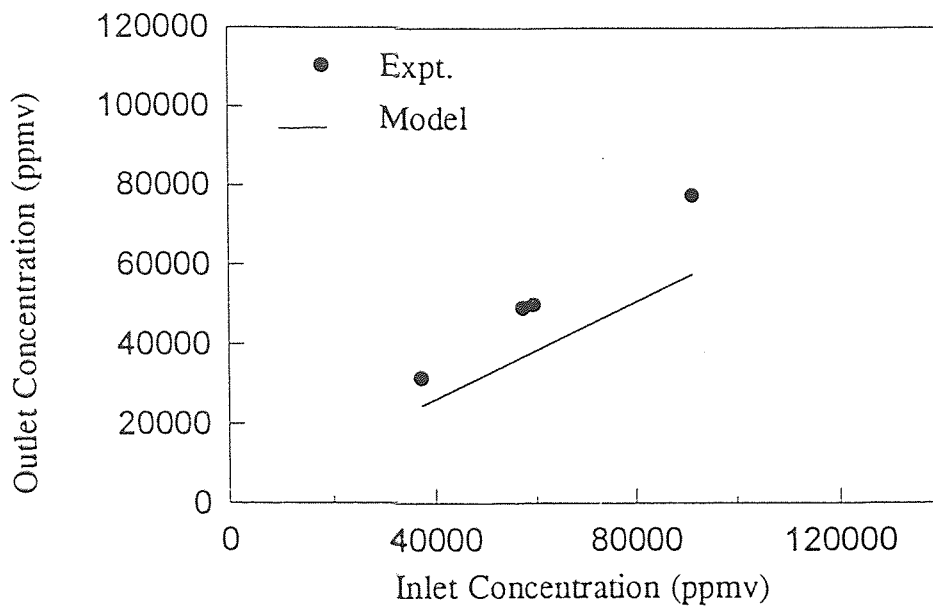
Feed Flow Rate: ~ 60 cc/min

Figure 37. Variation of Treated Gas Concentration with Feed Concentration
for Butane

Feed Concentration: 3.8% Pentane
96.2% Nitrogen
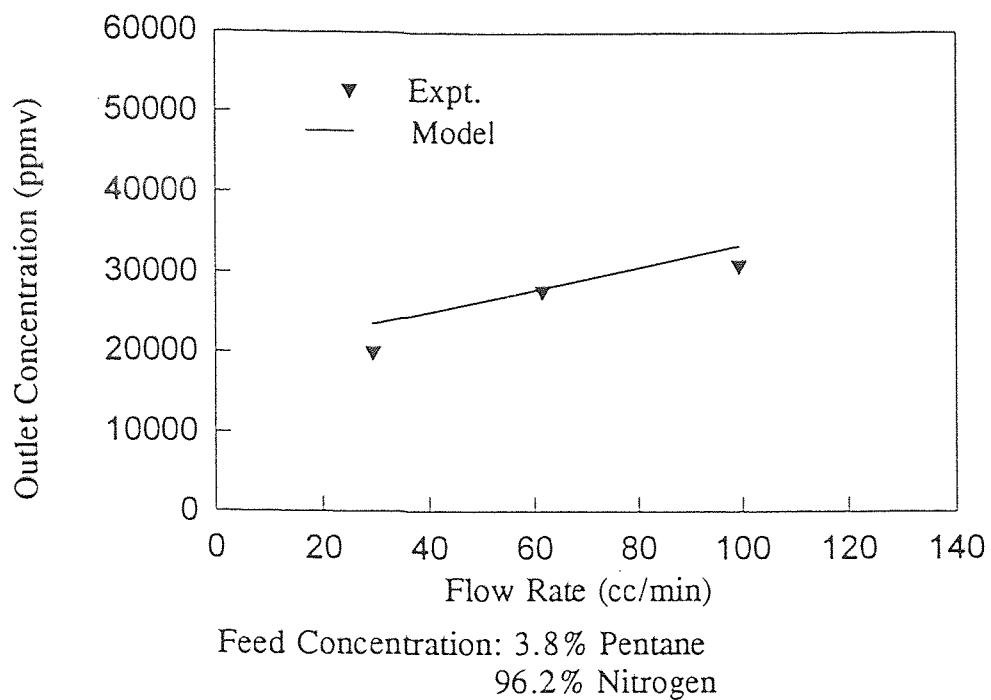
Figure 38. Comparison of Results for Pentane

Feed Flow Rate: ~ 60 cc/min

Figure 39. Variation of Outlet Concentration for Pentane

Figure 40. Dependence of Hexane Concentration on Flow Rate

Figure 41. Comparison of Experimental and Modeling Results for Variation of Hexane Concentration

CHAPTER 5

CONCLUSIONS

The following conclusions could be drawn from permeation/separation studies on gasoline vapor.

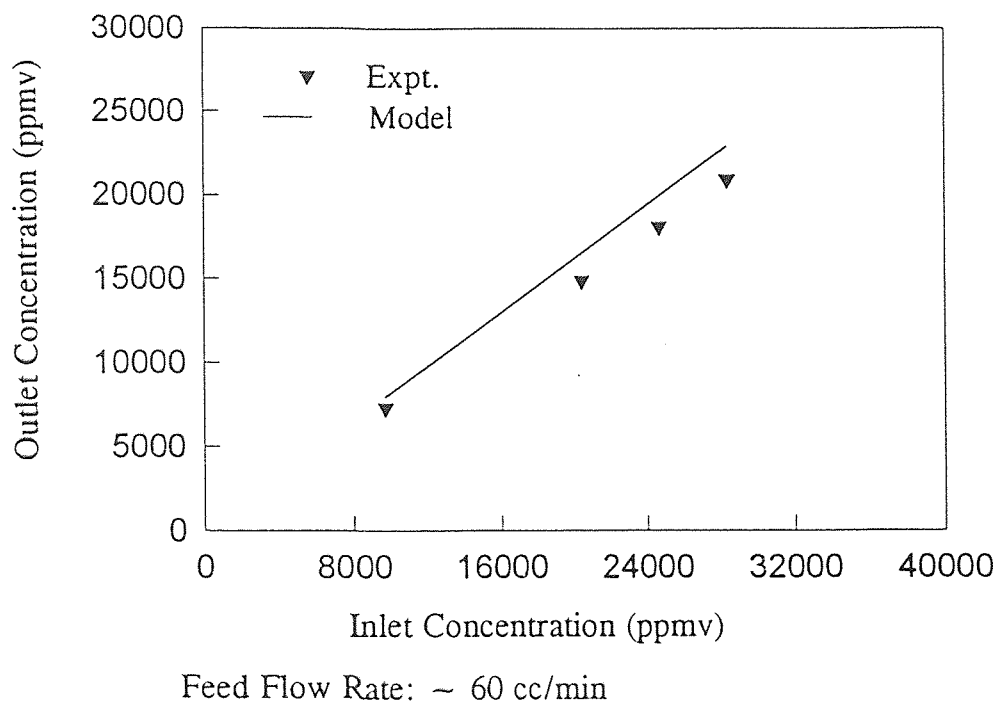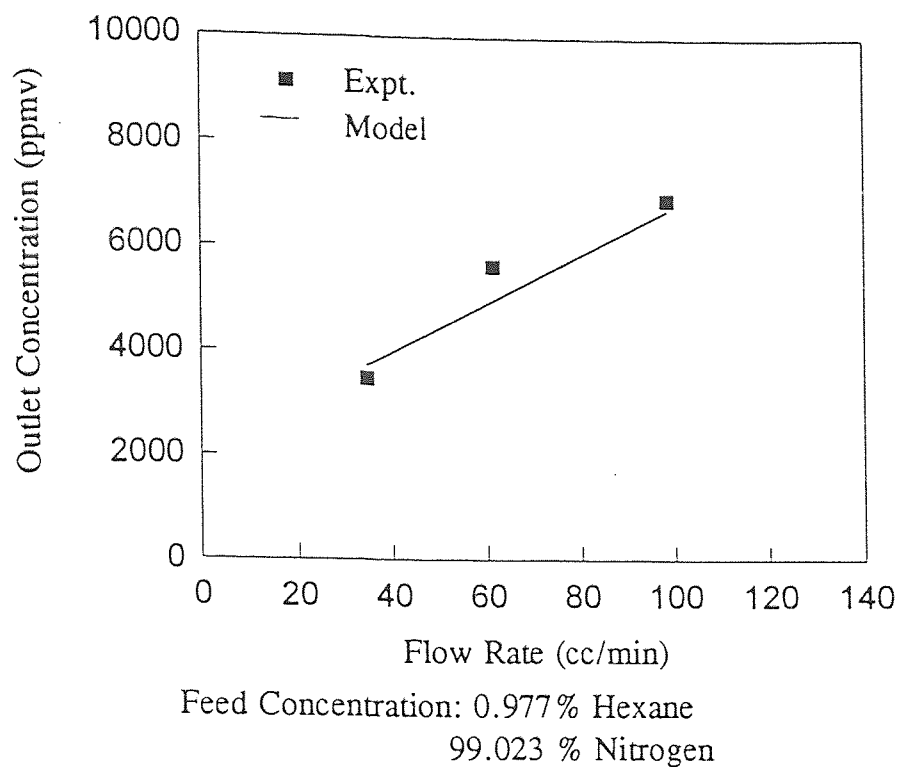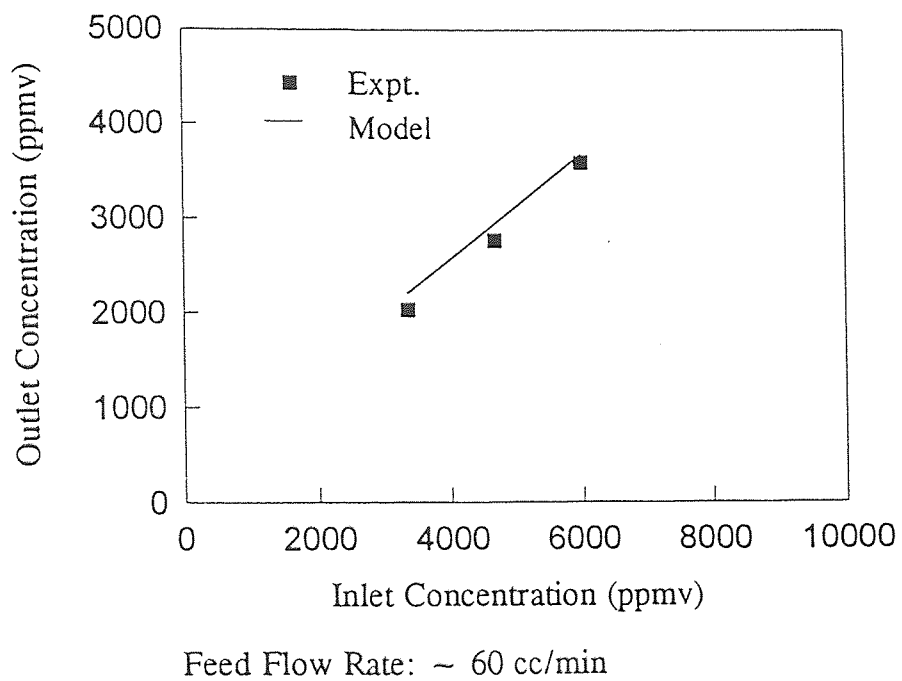1. Butane, pentane and hexane could successfully be removed at different concentrations, flow rates and permeate pressures using hollow fiber membranes with an ultrathin plasma polymerized silicone coating on the outer surface.

2. When the Celgard-based membranes and Mitsubishi-based membranes were used for hydrocarbon removal with an inert liquid immobilized in the pores, the separation performance of these membranes improved drastically. Separation factors increased by almost an order of magnitude, though the processing flow rates had to be kept very low. Therefore, ILMs are best suited for the kind of operation in which flow rates are low. It is necessary to have thinner ILMs to improve the module processing capacity.

3. Increasing the permeate pressure (i.e decreasing the vacuum level) from ~ 1.5 cm Hg to ~ 5.5 cm Hg did not affect the removal or selectivity to a very large extent.

4. The Mitsubishi-based membrane could be treated appropriately to yield the desired extent of separation and selectivity. This could be observed since there is a distinct difference between the performance of the membrane when the pores of the composite membrane were immobilized with a liquid, and the performance after the liquid was washed off from the pores.

5. The mathematical model developed has explained the difference in the two modes of

operation for methanol and toluene to a reasonable extent. However, experiments have to be done with binary mixtures (hydrocarbon and nitrogen) in the shell-side feed mode to check the applicability of the model for the hydrocarbons too.

6. Influence of the presence of other organics on permeation has been observed in separation studies done with model gasoline, but a detailed probe into such an effect (viz. presence of just one species, presence of two different species, presence of all three species etc.) was not carried out since it was not a part of this investigation. There is scope for more experimentation with a combination of any two of these hydrocarbons with nitrogen, with the distinct purpose of observing this effect.

APPENDIX A

SAMPLE CALCULATIONS

Sample calculations of flux, permeance, percent removal and selectivity for experimental data (data #4, Table 2) is shown in the following pages.

Feed gas flow rate(F_i): 27.62 cc/min.

Treated gas flow rate(F_o): 21.53 cc/min.

Feed concentration (X_{in}): 11.93% butane, 4.04% pentane, 0.998% hexane and 83.032% nitrogen.

Feed Pressure(P_f): 76 cm Hg

Treated gas concentration(X_{out}): 7.944% butane, 1.752% pentane, 0.226% hexane and 90.078% nitrogen.

Treated gas pressure(P_o): 76 cm Hg

Permeate pressure (P_p): 1.01 cm Hg

Temperature (T): 293.15 °K

Since calculations are similar for each of the three components, the routine for one component is shown here.

Permeate Flow Rate (F_p) = 27.62 - 21.53 = 6.09 cc/min

Concentration of butane in permeate (Y_p) = (27.62 x 11.93 - 21.53 x 7.944)/6.09

$$= 26.022\%$$

To calculate component flux:

The product of permeate flow rate (gmol/sec) and mole fraction of butane in permeate would yield permeate flux of butane.

Using PV=nRT, the volumetric flow rate can be converted to molar flow rate.

F_p = 6.09 cc/min x (76 cm Hg)/ ((6236.5 cc.cm Hg/gmol.°K) x 293.15 °K x 60 sec/min)

Molar permeate flow rate = 4.219E-6 gmol/sec

Permeate flux = Molar flow rate/Effective membrane area.

Effective membrane area = 3.14 x 290 x 10^{-4} cm x 25.4 cm x 50 = 115.6462 cm^2

Molar permeate flux = 4.219E-6/115.6462 = 3.65E-8 gmol/sec.cm^2

Butane permeate flux = 3.65E-8 x 0.26022 = 9.49E-9 gmol/sec.cm^2

Permeance = Permeate flux/Partial pressure difference

Since the partial pressure of butane varies throughout the module, a log mean value has to be calculated.

Partial pressure of butane on the feed side (upstream) = 76 x 11.93/100 = 9.067 cm Hg

Partial pressure of butane on the permeate side (upstream) = 1.01 x 26.022/100

$$= 0.263 \text{ cm Hg}$$

Partial pressure difference upstream (Δp_u) = 8.804 cm Hg

Partial pressure of butane on the feed side (downstream) = 76 x 7.944/100

$$= 6.037 \text{ cm Hg}$$

The partial pressure of butane in the downstream section of the permeate is very negligile compared to the upstream partial pressure. Hence, it is usually assumed as zero.

Partial pressure of butane on the permeate side (downstream) = 0

Partial pressure difference downstream (Δp_d) = 6.037 cm Hg

Log mean partial pressure difference $(\Delta p_{lm}) = (\Delta p_u - \Delta p_d)/ \ln (\Delta p_u/\Delta p_d)$

$$= 7.334 \text{ cm Hg}$$

Permeance of butane $(Q_b) = 9.49\text{E-}9/7.334 = 1.294\text{E-}9 \text{ gmol/sec.cm}^2.\text{cm Hg}$

Calculated in a similar manner,

Permeance of nitrogen $(Q_n) = 3.239\text{E-}10 \text{ gmol/sec.cm}^2.\text{cm Hg}$

Selectivity of butane (with respect to nitrogen) $= Q_b/Q_n = 1.294\text{E-}9/3.239\text{E-}10$

$$= 3.995$$

Percent removal of butane $= 1 - (21.53 \times 7.944/ 27.62 \times 11.93)$

$$= 48.09 \%$$

PROGRAM FOR SIMULATING RESULTS FOR METHANOL

```
C       DECLARE VARIABLES
        INTEGER ITMAX,N
        REAL ERREL,CFLOWMF
        PARAMETER (N=4)
C
        INTEGER K,I
        REAL FNORM,S,PHI
        REAL X(N),XGUESS(N)
        REAL XIN(101),LIN(101),XOUT(101),LOUT(101)
        REAL VOUT(101),YOUT(101)
        REAL PERM1(101),PERM2,PPERM(101),ALPHA(101)
        REAL BETA,PF,PERMF(101)
        REAL ERROR
C
        COMMON XIN(100),LIN(100),XOUT(100),LOUT(100),VOUT(100)
        COMMON YOUT(100)
        COMMON PERM1(100),PERM2,PPERM,ALPHA(100),BETA,PF,PVOC,I
        COMMON I,PF,PERM2,BETA,PPERM,XIN,LIN,ALPHA,PERM1
        COMMON PERMF,S,PHI
        EXTERNAL MODEL,NEQNF
        DATA XGUESS/0.4,0.039989,3.642E-11,8.314E-10/
C
        READ *, FIN,PPMVIN,PERFLOW,S,PHI
        I=1
        ERREL = 0.001
        ITMAX = 100
        ERROR=0.0
C
        DO WHILE (ERROR.LE.9.5E-1)
        LIN(1)=FIN*1.3401E-8
        XIN(1)=PPMVIN*1.0E-6
        PPERM(1)=0.1
        PERMF(1)=PERFLOW*1.3401E-8
C
        DO 10 I=1,100
        ALPHA(I)=267.7E-10*EXP(27.52*XIN(I))
        BETA=3.803E-10
```

79

```fortran
C     SETTING THE PERMEANCE VALUES
      PERM1(I)=ALPHA(I)
      PERM2=3.80303E-10

C     CONSTANT PRESSURE ON FEED SIDE
      PF=7.6E1

C               FIND THE SOLUTION
      CALL NEQNF(MODEL,ERREL,N,ITMAX,XGUESS,X,FNORM)
C     ASSUMING PORE RADIUS=50 Angstroms, THETA=0.3, TAU=6
C  S=PORE RADIUS(=50 ANGSTROMS)/PORE RADIUS(FOR SIMULATION)
C  S=20
C  PHI=FRACTION OF PORE THAT IS COATING DEPOSITED (=0.1)
      YOUT(I)=(X(1)*X(2)-X(3)*6280028.117*S*PHI)/PPERM(I)
      VOUT(I)=(X(3)+X(4))*2.0752e-2
      LOUT(I)=LIN(I)-VOUT(I)
      XOUT(I)=(LIN(I)*XIN(I)-VOUT(I)*YOUT(I))/LOUT(I)
      XIN(I+1)=XOUT(I)
      LIN(I+1)=LOUT(I)
      PPERM(I+1)=(1565994.17*PERMF(I)+(PPERM(I))**2)**0.5
      PERMF(I+1)=PERMF(I)-VOUT(I)
10    CONTINUE
      ERROR=(PERMF(100)-PERMF(101))/PERMF(100)
      PRINT *,'ERROR=',ERROR
      PERFLOW=FIN-(LOUT(100)/1.3401E-8)
      END DO
C      PRINT *,'I=',I
C      PRINT *,'FRAC=',FRAC
      PRINT *,'PPRIME(CM.HG)=',X(1)
      PRINT *,'Y1PRIME=',X(2)
      PRINT *,'FLUX N1(MOL/SQCM.SEC)=',X(3)
      PRINT *,'FLUX N2(MOL/SQCM.SEC)=',X(4)
      PRINT *,'PERMEATE PRESSURE AT CLOSED END=',PPERM(100)
      PRINT *,'PERMF(100)=',PERMF(100)
      PRINT *,'YOUT=',YOUT(100)
      PRINT *,'VOUT(100)=',VOUT(100)
      PPDROP1=X(1)*X(2)-PPERM(100)*YOUT(100)
      PRINT *,'PPDROP1=',PPDROP1
C      PRINT *,'FRAC=',FRAC
C      PRINT *,'PPDROP2(cmhg)=',X(1)*(1-X(2))-PPERM(100)*(1-YOUT(100))
      DRVFOR1=PF*XOUT(99)-PPERM(100)*YOUT(100)
      PRINT *,'TOTAL DRVFOR1=',DRVFOR1
      PRINT *,'DRVFOR1 ACROSS SKIN=',DRVFOR1-PPDROP1
```

```fortran
      PRINT *,'PPMVOUT=',XOUT(100)*1E6
      PRINT *,'FOUT=',LOUT(100)/1.3401E-8
      PRINT *,'PERMEATE FLOW RATE=',PERFLOW
      END
C
C

      SUBROUTINE MODEL(X,F,N)
      INTEGER N,I
      REAL F(N),X(N),S,PHI
      REAL PERM1(101),ALPHA(101),PPERM(101),PERMFLOW(101)
C
C
      REAL XIN(101),LIN(101),XOUT(101),LOUT(101)
      REAL VOUT(101),YOUT(101)
      COMMON I,PF,PERM2,BETA,PPERM,XIN,LIN,ALPHA,PERM1
      COMMON PERMFLOW,S,PHI
C     X(1)=PPRIME, X(2)=Y1PRIME, X(3)=N1,X(4)=N2
      F(1) = PERM1(I)*(PF*XIN(I)-X(1)*X(2))-X(3)
      F(2) = PERM2*(PF*(1.0-XIN(I))-X(1)*(1.0-X(2)))-X(4)
      F(3) = PERM1(I)*(1.0-X(2))*(PF*XIN(I)-X(1)*X(2))-PERM2*X(2)*
     & (PF*(1.0-XIN(I))-X(1)*(1.0-X(2)))
      F(4) = (X(3)*6280028.117*S*PHI)+(X(4)*5874428.402*S*PHI)-X(1)
     & +PPERM(I)
      RETURN
      END
```

APPENDIX C

PERMEANCE VALUES USED FOR MODELING

The experimentally obtained values of permeance for toluene, methanol, butane, pentane, hexane and nitrogen are reported in this appendix. The unit of permeance (Q_i/δ_c) is gmol/sec.cm^2.cm Hg and is related to the mole fraction (X_i) of each species through the functional dependence provided below.

Nitrogen:

$$Q_n/\delta_c = 3.803\text{E-}10$$

Toluene:

$$Q_t/\delta_c = 185.65\text{E-}10 \times \text{EXP} \, (78.81 \times X_t)$$

Methanol:

$$Q_m/\delta_c = 267.70\text{E-}10 \times \text{EXP} \, (27.52 \times X_m)$$

Butane:

$$Q_b/\delta_c = 2.534\text{E-}9 + 2.412\text{E-}9 \times X_b + 2.1689\text{E-}8 \times X_b^2$$

Pentane:

$$Q_b/\delta_c = 1.290\text{E-}9 + 7.530\text{E-}9 \times X_p + 1.1115\text{E-}7 \times X_p^2$$

Hexane:

$$Q_b/\delta_c = 2.264\text{E-}9 + 9.479\text{E-}9 \times X_h + 9.9739\text{E-}6 \times X_h^2$$

REFERENCES

Baker, R.W. and Wijmans, J.G., "Membrane Separation of Organic Vapors from Gas Streams", Chapter 8 in *Polymeric Gas Separation Membranes*, edited by Paul, D.R. and Yampol'skii, Y.P., pp 353-397, CRC Press, Boca Raton, FL, 1994.

Baker, R.W., Yoshioka, N., Mohr, J.M. and Khan, A.J., "Separation of Organic Vapors from Air", J. Memb. Sci, 31, 259, 1987.

Bhave, R.R. and Sirkar, K.K., "Gas Permeation and Separation by Aqueous Membrane Immobilized across the Whole Thickness or in a Thin Section of Hydrophilic Microporous Celgard Films,", J. Memb. Sci., 27, 41, 1986.

Cha, J.S., "Removal of Vapors from Air by Selective Membrane Processes", a Ph.D. Dissertation, Dept. of Chem. Engg., New Jersey Institute of Technology, Newark, NJ, 1994.

Deng, S., Sourirajan, A., Matsuura, T. and Farnand, B., "Study of Volatile Hydrocarbon Emission Control by an Aromatic Poly(ether imide) Membrane", Ind. Eng. Chem. Res., 34, pp 4494-4500, 1995.

Humphrey, J.L. and Associates, "Separation Processes: Playing a Critical Role", Chem. Eng. Prog., pp 31-41, October, 1995.

Kimmerle, K., Bell, C.W., Gudernatch, G. and Chmiel, H., "Solvent Recovery from Air", J. Memb. Sci., 36, 577, 1988.

Malik, V., "Removal of VOCs from a Waste Gas Stream by a Hollow Fiber Permeator", Master's Thesis, Dept. of Chem Engg., New Jersey Institute of Technology, Newark, NJ, 1995.

Matson, S.L., Herrick, C.S. and Ward, W.J., "Progress on the Selective Removal of H_2S from Gasified Coal Using an Immobilized Liquid Membrane", Ind. Eng. Chem. Process. Des. Dev., 16, 370, 1977.

Ohlrogge, K., Peinemann, K. V., Wind, J. and Behling R.D., "The Separation of Hydrocarbon Vapors with Membranes", Sep. Sci. and Tech., Vol. 25 (13-15), 1990.

Ohlrogge, K., Wind, J. and Behling, R.D., "Off-gas Purification by Means of Membrane Vapor Separation Systems", Sep. Sci. and Tech., Vol. 30 (7-9), 1625-1638, 1995.

REFERENCES
(Continued)

Pan, C.Y. and Habgood, H.W., "Gas Separation by Permeation. Part II: Effect of Permeate Pressure Drop and Choice of Permeate Pressure", The Can. J. of Chem. Eng., Vol. 56, April 1978.

Papadopoulos, T., "Further Studies on Hollow Fiber Contained Liquid Membrane Separation of Gas and Liquid Mixtures", a Ph.D. Dissertation, Dept. of Chem. Engg., Stevens Institute of Technology, Hoboken, NJ, 1992.

Peinemann, K.V., Mohr, J.M. and Baker, R.W., "The Separation of Organic Vapors from Air", AIChE Symp. Series., 82 (250), 19, 1986.

Sengupta, A. and Sirkar, K.K., "Membrane Gas Separation" in Progress in Filtration and Separation; Wakeman, R.J., Ed.; Elsevier, Amsterdam, Vol.4, p 289, 1986.

Strathmann, H., Bell, C.M. and Kimmerle, K., "Development of Synthetic Membranes for Gas and Vapor Separation", Pure and Appl. Chem., 58, No.12, 1663-1668, 1986.

Ward, W.J. and Robb, W.L., "Carbon Dioxide - Oxygen Separation: Facilitated Transport of Carbon Dioxide Across a Liquid Film", Science, 156, 1481, 1967.

Wijmans, J.G. and Helm, V.D., "A Membrane System for the Separation and Recovery of Organic Vapor Streams from Gas Streams", AIChE Symp. Series 272.85, 1989, 74-79.

Xomeritakis, G. and Lin, Y., "Chemical Vapor Deposition of Solid Oxides in Porous Media for Ceramic Membrane Preparation. Comparison of Experimental Results with Semianalytical Solutions", Ind. Eng. Chem. Res., Vol. 33, 2607-2617, 1994.